

1 The missing *Myopus*: plugging the gaps in Late Pleistocene small  
2 mammal identification in western Europe with geometric  
3 morphometrics

4 Louis Arbez<sup>1,2, a</sup>, Aurélien Royer<sup>2</sup>, Danielle Schreve<sup>3</sup>, Rémi Laffont<sup>2</sup>, Serge David<sup>4</sup>, Sophie  
5 Montuire<sup>1,2</sup>

6

7 <sup>1</sup> EPHE, PSL University, 6 Boulevard Gabriel, 21000 Dijon, France;

8 <sup>2</sup> Biogéosciences, UMR 6282, CNRS, EPHE, Université Bourgogne Franche-Comté, 6  
9 Boulevard Gabriel, 21000 Dijon, France;

10 <sup>3</sup> Department of Geography, Royal Holloway University of London, Egham, Surrey TW20  
11 OEX, UK;

12 <sup>4</sup> CJP - Centre Jurassien du Patrimoine, 2, place de l'Hôtel de Ville 39000 Lons-le-Saunier;

13 <sup>a</sup> Louis.Arbez@u-bourgogne.fr.

14 Abstract word count: 205

15 Main text word count: 7424

16 Figures: 6

17 Tables: 4

18 Bibliography: 3047 words, 104 references

19 Annexes: 1 table

## 20 **Abstract**

21 *Lemmus* and *Myopus* are two lemming species with distinct habitat requirements but which  
22 show very similar dental morphologies. They are thus extremely difficult to distinguish from  
23 one another in the fossil record on the basis of their dental remains, leading to poor  
24 understanding of the palaeobiogeographical evolution of *Myopus* as well as inaccurate  
25 paleoenvironmental reconstructions. Currently, the presence of *Myopus* in the fossil register  
26 from the Pleistocene is still debated and no firm occurrence of this lemming in western Europe  
27 has yet been confirmed during the Late Pleistocene. In this paper, we used geometric  
28 morphometrics on modern material to establish morphological differences between *Lemmus*  
29 and *Myopus* teeth (first lower and third upper molars). Morphological data was then used to  
30 build a robust linear discriminant model able to confidently classify isolated teeth of these two  
31 genera, and finally, linear discriminant models were used on fossil remains of *Lemmus/Myopus*  
32 from two Late Pleistocene archaeological/palaeontological sites (Grotte des Gorges and Gully  
33 Cave). This study demonstrates, for the first time, the presence of *Myopus schisticolor* in west  
34 European Late Pleistocene sites between the end of MIS 3 and the beginning of Holocene,  
35 during climatic events that favoured the development of taiga forest of birch and pine in these  
36 regions.

## 37 **Keywords**

38 Geometric morphometrics, Lemming, Late Glacial, Paleobiogeography, Molar shape, Boreal  
39 environment, Taxonomy

## 40 **1. Introduction**

41 Rodents are characterized by a significant taxonomic diversity associated with various  
42 ecological and biological traits, thereby ensuring their widespread occurrence throughout all  
43 modern biotopes. They have been intensively studied with respect to the fields of evolution,

44 biochronology and palaeoenvironmental change (e.g. Chaline and Mein, 1979; Cox and  
45 Hautier, 2015; Fejfar and Heinrich, 1990; Hernandez Fernandez, 2006; van Kolfschoten, 1995;  
46 Kowalski, 1995; Montuire et al., 1997; Rekovets and Kovalchuk, 2017). Their remains, well  
47 preserved in many archaeological and palaeontological contexts, have therefore contributed to  
48 the reconstruction of patterns of Quaternary palaeoclimatic change, still a major challenge in  
49 our understanding of continental chronostratigraphies today. Among the methods applied for  
50 paleoclimate reconstructions, many are based on species associations, such as the  
51 presence/absence or relative abundance of species, hence the need to have accurate taxonomic  
52 identifications (e.g. Gobalet 2001; Lyman, 2002, 2019; Royer et al., 2020; Stahl, 1996).

53 Numerous obstacles hinder the identification of small-bodied animals, even when their skeletal  
54 remains are recovered (Stahl, 1996). One problem is that while modern zoologists have many  
55 criteria by which to identify animals (e.g. fur, size, skull and post-cranial anatomy, geographical  
56 range), most of these criteria cannot be applied to fossils. A second problem is that identification  
57 of small mammals is based on limited types of remains, generally the teeth, which are most  
58 resistant to mechanical taphonomical processes. Despite dental remains being the most  
59 diagnostic elements at the genus or species levels, teeth may exhibit very similar morphologies,  
60 which could potentially prevent confident identifications. The last problem also reflects the  
61 differential state of diagnostic information for relevant taxa (Lyman, 2019; Stahl, 1996). Many  
62 criteria have been proposed to identify these smallest-size species, but most of them rely on the  
63 “holotypic” morphology (i.e. the typical form as defined by characteristic specimens of this  
64 species), without taking into account geographical or inter-population variability, except to  
65 point out very unusual cases. The ensuing large number of criteria proposed for species  
66 identification often leads either to disagreement or to differential use of these criteria among  
67 taxonomists. As said by Stahl (1996), it must always be remembered that higher level  
68 taxonomic categories are necessarily dynamic and constantly open to revision.

69 Among the rodents, voles and lemmings, which show substantial tooth variability throughout  
70 species, time and space, are key taxa for tracking Quaternary environmental and climatic  
71 changes (e.g. Kowalski, 2001; Montuire et al., 2019; Nadachowski 1982; Royer, 2013).  
72 Lemmings are reliable biomarkers of specific and typical high latitude environments (Chaline,  
73 1972; Kowalski, 1995). In Eurasia, four lemming genera are found in fossil contexts: 1)  
74 *Dicrostonyx* and *Lagurus*, which are regularly present during the coldest or driest phases of the  
75 Late Pleistocene extending as far as the south of France (Chaline, 1972; Marquet, 1993; Royer  
76 et al., 2016); 2) *Lemmus*, which is also frequently found throughout Eurasia in open and cold  
77 environments, but still in modest abundance (Kowalski, 1995, 2001), and 3) *Myopus*, which  
78 has so far only been attested in Russia at this time, associated with more temperate species (e.g.  
79 Markova et al., 2019; Ponomarev et al., 2013a, 2013b, 2013c).

80 As *Lemmus* (Link, 1795) and *Myopus* (Miller, 1910) have two strong but divergent ecological  
81 signals, their taxonomic discrimination in the fossil assemblages is essential in order to  
82 investigate past faunal associations and understand their significance in paleoclimatic  
83 reconstructions. The True Lemming genus (*Lemmus*) is a complex of several species which  
84 have a northern distribution restricted to Arctic tundra environments associated with high  
85 seasonality and little vegetation. These taxa use the thick snow covering as a shelter, giving  
86 them access to the vegetation persisting under this natural shield during winter (Domine et al.,  
87 2018; Reid et al., 2011; Stenseth and Ims, 1993), as well as using bogs and wetlands during  
88 summer and eschewing forest as much as possible (Le Vaillant et al., 2018; Wilson et al., 2017).  
89 The wood lemming (*Myopus schisticolor* [Lilljeborg, 1844]) is the only representative of its  
90 genus and inhabits exclusively coniferous forest with a thick moss cover, which constitutes its  
91 main food source (Bobretsov and Lukyanova, 2017; Calandra et al., 2015; Eskelinen, 2002).  
92 Contrary to *Lemmus*, this taxon avoids bogs and marshes and is present throughout the taiga  
93 forests from Scandinavia to the eastern coast of the Sea of Okhotsk.

94 Although *Myopus* and *Lemmus* are separated by a large phylogenetic distance (Abramson and  
95 Petrova, 2018) and are easily distinguishable in their external appearance (Gromov and  
96 Polyakov, 1992; Wilson et al., 2017), they express a great deal of similarity in terms of their  
97 dental morphology (Borodin, 2009; Chaline et al., 1988; Koenigswald and Martin, 1984;  
98 Kowalski, 1995), resulting in their fossil remains often being impossible to separate or being  
99 lumped together as “*Lemmus-Myopus*” (Kowalski, 2001). This problem of differentiation has  
100 therefore greatly reduced the palaeoecological utility of these taxa, which is particularly  
101 problematic considering their occurrence in many Quaternary deposits. Several authors have  
102 accordingly attempted to separate these two genera through morphometrical analysis of the first  
103 lower molar (m1) and the third upper molar (M3) but with varying degrees of accuracy (Chaline  
104 et al., 1988; Markova et al., 2018; Ponomarev et al., 2013b; Smirnov et al., 1997).

105 The present paper aims to resolve this problem by providing a robust means of differentiating  
106 between the teeth of these two genera, *Lemmus* and *Myopus*. This study uses geometric  
107 morphometrics, which has never been applied on these two genera, despite its efficiency in  
108 identifying similar species in modern and fossil record (e.g. McGuire, 2011; Cucchi et al., 2014;  
109 Hulme-Beaman et al., 2018; Stoetzel et al., 2017; Navarro et al., 2018; Kolendrianou et al.,  
110 2020). Several modern populations were considered, both to establish differences in their dental  
111 morphologies and to evaluate the reliability of traditional criteria previously used to separate  
112 the two genera. The geometric morphometric approach is then coupled with a discriminant  
113 function analysis in order to separate these two genera before being applied to European fossil  
114 specimens from two Late Pleistocene sites. The outcomes of this paper consequently propose  
115 not only a novel and replicable means of identifying and separating the two genera, but also  
116 allow a new view of the past environments and biogeographical evolution of lemming  
117 populations.

## 118 2. Taxonomy and Morphology

119 *Lemmus* and *Myopus* genera belong to the tribe Lemmini (Gray, 1825), which is part of the  
120 Arvicolinae subfamily (Gray, 1821). The genus *Lemmus* is currently divided into four distinct  
121 species (Abramson and Petrova, 2018; Wilson et al., 2017): the Nearctic North American brown  
122 lemming *Lemmus trimucronatus* (Richardson, 1825) and the Palearctic Norway lemming  
123 *Lemmus lemmus* (Linnaeus, 1758), Siberian lemming *Lemmus sibiricus* (Kerr, 1792) and the  
124 Amur lemming *Lemmus amurensis* (Vinogradov, 1924). Originally, *Myopus* was recognized as  
125 a member of the genus *Lemmus* and named as *Lemmus schisticolor* (Lilljeborg, 1844) due to  
126 osteological similarities, such as the general shape of the skull (Ognev, 1948), the convergence  
127 of the maxillary tooth rows and the inclination of the mandibular tooth rows (Abramson, 1993).  
128 Miller (1910, 1912) separated *Myopus* from *Lemmus*, leading to the recognition of *Myopus*  
129 *schisticolor*, a species characterized by a combination of *Lemmus* characters (skull and teeth)  
130 and vole characters (general body-form and foot structure). Recent DNA studies clearly attest  
131 to the separation of these two genera (Abramson and Petrova, 2018; Buzan et al., 2008; Cook  
132 et al., 2004; Robovský et al., 2008).

133 Molars of *Lemmus* and *Myopus* are hypsodont with a flat grinding surface and have a prismatic  
134 structure composed of alternate triangles and deep re-entrant angles filled with cement (fig. 1).  
135 The first lower molar (m1) is constituted by a posterior loop (PL), three closed alternating  
136 triangles (T1-T3), two confluent triangles (T4 and T5) and an anterior loop (AL). The third  
137 upper molar (M3) shows a similar structure (fig. 1), with an anterior loop, five triangles and a  
138 posterior loop (PL). For these two molars, some authors note a high variation in the outer loops  
139 (anterior loop for m1, posterior loop for M3), which exhibit different stages of complexity, with  
140 the development of supplementary re-entrant angles on both labial and buccal sides (e.g.  
141 Markova et al., 2018; Ponomarev et al., 2013b). In general, *Lemmus* shows a higher tendency  
142 to complexity (i.e. development of supplementary re-entrant angles) and *Myopus* has a simpler

143 morphology. However, due to a large overlap, these trends cannot be used to definitively  
144 attribute individuals to one or the other of these genera. Based on biometrical approaches, linear  
145 measurements are the most commonly used features to distinguish these two genera on isolated  
146 teeth (*e.g.* Borodin, 2009; Ponomarev et al., 2013b; Roberts and Parfitt, 1999; Tiunov and  
147 Panasenکو, 2011), with the following features identified as being of potential significance: 1)  
148 differences in the length/width ratio of M3 (Smirnov et al., 1997), with the M3 shape in *Myopus*  
149 tending to be more compact and that in *Lemmus* tending to be more elongated; 2) ratios obtained  
150 from several linear measurements to characterize the global shape of the different molars  
151 (Chaline et al., 1988); and 3) the size of the teeth, with a greater tooth length in *Lemmus* (Chaline  
152 et al., 1988; Smirnov et al., 1997). Finally, a supplementary criterion based on cementum was  
153 recently proposed by Ponomarev et al. (2013b). This last work shows that the frequency of  
154 cementum deposits in the last re-entrant angles of the outer loops of both M3 and m1 (LRA3  
155 and BRA4 of m1) differs between the two genera. The cementum deposits are absent in *Myopus*  
156 teeth, whereas they are present in 40 to 70% of *Lemmus* individuals (Cheprakov, 2016; Markova  
157 et al., 2018; Ponomarev et al., 2013).

### 158 **3. Materials and methods**

#### 159 3.1. Modern specimens

160 Since the focus of this paper is the application of the geometric morphometrics method to  
161 western European fossil sites, modern *Lemmus* and *Myopus* individuals were targeted from  
162 Scandinavia and Russia. The modern samples are composed of research laboratory collections  
163 and Snowy Owl (*Bubo scandiacus*) pellets and are housed in the research laboratory collections  
164 in Biogéosciences at the University of Burgundy and in the Arctic Research Station of  
165 Labytnangi in Russia. In total, 30 *Myopus* and 96 *Lemmus* m1 specimens, and 31 *Myopus* and  
166 91 *Lemmus* M3 specimens were analysed (see table 1 for details). Since the *Myopus* genus is  
167 monospecific, our sample was only composed of individuals of *Myopus schisticolor*. To

168 describe most of the current morphological variability of the *Lemmus* genus, our sample  
169 included specimens from the three different species. Most of our sample belong to two  
170 palearctic species, with 50 Norway Lemming (*L. lemmus*) and 34 western Siberian Lemming  
171 (*L. sibiricus*). The two species are closely related in their phylogeny but were already separated  
172 during the Late Pleistocene (Abramson and Petrova, 2018). Few individuals of eastern *L.*  
173 *sibiricus* from Chukotka district were included to capture the range of potential variability of  
174 the genus. Additionally, 12 m1 and 8 M3 of North American Brown Lemming (*L.*  
175 *trimucronatus*) were included to clarify the distinction amongst the different representatives of  
176 *Lemmus*. Numbers and origins of the specimens are detailed in table 1 and figure 2. Only well-  
177 preserved and complete molars were used in the analyses; all broken and digested teeth were  
178 discarded.

### 179 3.2. Fossil samples

180 Fossil specimens come from two archaeological/palaeontological sites from Late Pleistocene,  
181 la Grotte des Gorges (France) and Gully Cave (England) (fig. 2). As for the modern material,  
182 broken and digested teeth were not included in this study. All dates of la Grotte des Gorges  
183 have been calibrated using IntCal13 (Reimer et al., 2013).

184 **La Grotte des Gorges** is located close to Amange village (Jura, France) and was excavated  
185 between 2008 and 2017. Two layers (1a and 1b) yielded archaeological material (David et al.,  
186 2014, 2017), from the end of MIS 3 with AMS dates ranging from  $33,030 \pm 750$  to  $29,390 \pm$   
187  $170$  uncal. BP. The site yields a diverse association of mammalian species demonstrating a  
188 transition from arctic toward steppe environment. *Lemmus/Myopus* remains come from the  
189 upper part of the sequence (layer 1a), dominated by typical taxa of cold-climate phases such as  
190 reindeer (*Rangifer tarandus*), mammoth (*Mammuthus primigenius*), rhinoceros  
191 (Rhinocerotidae) and collared lemmings (*Dicrostonyx torquatus*) The second phase of the  
192 sequence (layer 1b) is dominated by bison (*Bison priscus*), which is typical taxa of steppe



193 environment. A total of 11 first lower and 3 third upper molars attributed to *Lemmus/Myopus*  
194 has been analysed (table 1 and figure 2).

195 **Gully Cave** is located in Ebbor Gorge (Somerset, UK) and has been the subject of ongoing  
196 excavation since 2006. The upper stratigraphic units (of relevance here) consist of matrix-rich  
197 limestone breccias of Lateglacial Interstadial and Holocene age respectively, separated by a  
198 coarse, open-framework limestone breccia deposited during the Younger Dryas, the  
199 stratigraphy underpinned by radiocarbon dates on mammalian faunal remains from throughout  
200 the sequence. The cave was completely filled by around 10,000 cal years BP and the sequence  
201 was capped by a discontinuous flowstone. A total of 35 m1 teeth were analyzed, 12 from the  
202 Younger Dryas levels (date range 12409-12037 cal. BP to 11950-11259 cal. BP) and the other  
203 23 from the boundary level between the Allerød interstadial and the Younger Dryas (date range  
204 12379-12637 cal. BP to 13214-13444 cal. BP), and 43 M3s, with 17 from the Younger Dryas  
205 and 26 from the Allerød interstadial-Younger Dryas transition. The mammalian assemblage  
206 from the Younger Dryas levels sampled here includes *Lepus timidus*, *Myodes* sp., *Dicrostonyx*  
207 *torquatus*, *Lemmus/Myopus*, *Microtus agrestis* or *arvalis*, *Lasiopodomys gregalis*,  
208 *Alexandromys oeconomicus*, *Vulpes* sp. and *Rangifer tarandus*. The sample from the Allerød  
209 interstadial-Younger Dryas transition has yielded *L. timidus*, *Ochotona pusilla*, *Arvicola*  
210 *amphibius*, *Clethrionomys glareolus*, *D. torquatus*, *Lemmus/Myopus*, *M. agrestis* or *arvalis*, *L.*  
211 *gregalis*, *Al. oeconomicus*, *V. lagopus*, *R. tarandus* and *Cervus elaphus*.

### 212 3.3. Landmark schemes and data acquisition

213 All teeth were photographed using a macro objective (Canon EOS6D mark II, macroscopic  
214 objective MP-E 65mm f/2.8) and saved in .jpg format with a 72-dpi resolution. To avoid  
215 between-picture deformation, all specimens were photographed one by one with the same  
216 distance from the objective and with the same focus. Outlines were then extracted from pictures  
217 using ImageJ v.1.52a. The m1 outline was then orientated with a manual marking of two

218 landmarks (Lm 3 and 7, fig. 1), which define the tooth's vertical axis, in order to correctly  
219 position the tooth following the protocol of Navarro et al. (2018). No satisfactory orientation  
220 could be obtained with this protocol on the M3, so the procedure was adapted as follows. The  
221 outline pixels were rotated along the first principal component axis of the outline pixel  
222 coordinate matrix. These standardized orientations then enabled landmarks located at the  
223 extreme tips of the salient and reentrant triangles to be automatically detected, as well as those  
224 at the extreme tips of the posterior and anterior loops. All landmarked teeth were further  
225 inspected for gross error, and the entire procedure was performed by a single operator, thereby  
226 avoiding inter-operator biases.

227 In total, seven landmark schemes and two biometric measurements were defined to describe  
228 the morphological variability of the m1 and M3 (table 2 and fig.1). The global shape of each  
229 tooth was analysed with a fixed landmark scheme (**FL**), using 14 landmarks for the m1 (**m1-**  
230 **FL**) and 11 landmarks for the M3 (**M3-FL**). A total of 20 semi-landmarks for m1 and 50 semi-  
231 landmarks for M3 were used to characterize the outer loops (anterior loop dataset **m1-AL** and  
232 posterior loop dataset **M3-PL**). The **SL** schemes, **m1-SL** and **M3-SL** correspond to FL datasets  
233 combined with semi-landmarks of outer loops (**m1-AL** or **M3-PL**). Another semi-landmark  
234 scheme describes the alternation between T2 and T3 of M3 (**M3-TR**) by using a total of 4 fixed  
235 landmarks and 30 semi-landmarks. In all semi-landmark configurations, few fixed landmarks  
236 were removed to treat whole loops only using semi-landmarks (landmark removed for each  
237 dataset: **m1-SL/AL**: Lm8, 9, 10; **M3-SL/PL**: Lm 9, **M3-TR**: Lm3).

238 In addition, the tooth length (**TL**) of the two teeth was estimated based on the Euclidean distance  
239 between the most anterior and posterior landmarks (Lm1 and 9 for m1; Lm1 and 7 for M3).

#### 240 3.4. Geometric morphometrics

241 All configurations of each landmark dataset (**m1-FL**, **m1-SL**, **m1-AL**, **M3-FL**, **M3-SL**, **M3-**  
242 **PL**, **M3-TR**) were superimposed using partial Generalized Procrustes Analysis (GPA),

243 performed independently for each dataset. This procedure aims to separate the shape component  
244 from the position, size and orientation components contained within the coordinates of  
245 landmark configurations. GPA proceeds by 1) translating each individual configuration so that  
246 their centroids coincide, 2) scaling each landmark configuration to unit centroid size, and 3)  
247 rotating each configuration onto the dataset mean shape by minimizing Procrustes distances  
248 between each configuration and this mean shape (Dryden and Mardia, 1998; Rohlf and Slice,  
249 1990; Zelditch et al., 2012). For **m1-SL**, **m1-AL**, **M3-SL**, **M3-PL** and **M3-TR**, semi-landmarks  
250 are allowed to slide to minimize the bending energy between the specimen configurations and  
251 the meanshape of the dataset under consideration (Bookstein, 1997).

252 The obtained coordinates (Procrustes coordinates) were then projected onto the Euclidean  
253 tangent space (the tangent point being the mean shape of the dataset). These tangent space  
254 coordinates are finally rotated by a Principal Component Analysis (PCA) to keep only principal  
255 components with non-null eigenvalues (the rank deficient nature of tangent space data resulting  
256 from loss of degree of freedom during GPA, and, in our case, to some datasets with fewer  
257 individuals than shape variables). For each dataset, a few outliers were identified as those  
258 individuals with high Procrustes distances compared to their mean shape (i.e. lying beyond the  
259 third quartile increased by 1.5 times the interquartile range) and were sequentially removed  
260 after a new GPA (table 2).

261 In order to avoid any influence of fossil specimens on the molar shape variation depicted by the  
262 tangent space, which was then used to build the discriminant model among both genera, we  
263 treated fossil specimens as supplementary specimens in our analyses (see Navarro et al. 2018).  
264 Fossil specimens were so aligned on the modern mean shape so that, for a given dataset, they  
265 lay on the same shape and tangent spaces as the modern individuals. Then, the rotation  
266 computed on the tangent space for the modern individuals was used to rotate the projection of  
267 fossil specimens in the same way.

268 All geometric morphometrics analyses were performed with the geomorph package version  
269 3.2.0 on R v3.6.2 (R Core team, 2019).

### 270 3.5. Statistical classification

271 The predictive model was built using linear discriminant analysis (LDA) quantifying the shape  
272 differences between the two genera (*Myopus* vs *Lemmus*), and the quality of the obtained model  
273 was assessed by Leave-One-Out Cross-Validation (LOOCV). This procedure removes one  
274 specimen from the sample at a time and predicts its classification between groups using LDA  
275 functions calculated on the remaining specimens. Then, the removed specimen is classified by  
276 a new function, computed using data that do not take the specimen into consideration, thereby  
277 reducing potential inflation of the prediction error and avoiding issues of circular reasoning and  
278 over-fitting problems (Kovarovich et al., 2011).

279 LDA can be extremely sensitive to the relation between the number of groups, the number of  
280 predictor variables and the total sample size. As rule-of-thumb, the total number of predictor  
281 variables needs to be smaller than the sample size of the smallest predicted group (Kovarovich  
282 et al., 2011). Special attention has been paid to this rule due to our small sample size and the  
283 high number of predictor variables. Firstly, we reduced the number of predictors used to build  
284 the discriminant functions by applying the method of Baylac and Friess (2005). This method  
285 substitutes primary data (Procrustes coordinates) by PCs scores to build the model. This was  
286 done by building each model and its LOOCV based on the first  $k$  PCs, with  $k$  varying from 1 to  
287  $p$  ( $p$  being the sample size of the smallest group under consideration). The optimal number of  
288 PCs for the most efficient model was determined by the lowest prediction error rate (i.e. the  
289 maximum number of correctly assigned specimens).

290 Secondly, the method of Evin et al. (2013) was used to evaluate possible biases due to our  
291 unbalanced dataset. For a given unbalanced dataset, 100 balanced samples were built by  
292 randomly picking a subset of individuals from the largest group, and for each such sample,

293 LDA was computed. The observed classification score for each unbalanced dataset was then  
294 compared with these 100 balanced samples. Models were also compared with the null  
295 hypothesis of no shape difference between genera (hence the classification would be only due  
296 to chance, resulting in a 50% error rate). 100 such null models were generated for balanced  
297 samples of the two species by randomly reassigning specimens to genera. Finally, the quality  
298 of the models was evaluated by checking at posterior probabilities of correctly assigned genus  
299 for each dataset.

300 All codes including automatic landmark placement and data treatment are available on request.

## 301 **4. Results**

### 302 4.1. Morphospaces and morphological variation

#### 303 4.1.1. The first lower molar

304 In the tooth shape analyses (**m1-FL**, **m1-SL** and **m1-AL**), the two first PCs account,  
305 respectively, for 32.6%, 56.6% and 69.6% of the explained variance (table 3, fig. 3). The  
306 number of PCs explaining at least 90% of the initial shape variation is 13, 12 and 6, respectively.  
307 For the **m1-FL** configuration, shape changes mainly concern the buccal triangles (T2-T4)  
308 shifting labially and the Lm1 and 9 shifting laterally. For the **m1-SL**, the main behaviour is  
309 focused on the anterior loop, which tends to roundness enhancing the confluence of T4/T5 (fig.  
310 3B). The shape variation on **m1-AL** exhibits a more pronounced development of the re-entrant  
311 angles (fig. 3C). The most important part of the variation is expressed by PC1 and tends to  
312 separate the two genera for all datasets, with the least overlap for the **m1-SL** analysis and the  
313 largest one for the **m1-FL** (fig. 3A). On the two first PCs from these three landmark schemes,  
314 one can note no specific distinction between *Lemmus* species (fig. 3). The tooth lengths of  
315 *Lemmus* and *Myopus* range from 1.6 to 2.4 mm and from 1.4 to 1.7 mm, respectively (fig. 3H).  
316 A large overlap in the tooth length range is observed between the two genera, with 86% of the

317 *Myopus* specimens being included within *Lemmus*'s tooth length range. Within the *Lemmus*  
318 genus, *L. sibiricus* is the species which has the longest tooth length compared to the two others.

#### 319 4.1.2. The third upper molar

320 The same pattern as m1 is observed on the M3 with the first two PCs explaining 46.1%, 70.0%,  
321 75.7% and 57.7% of variation respectively **M3-FL**, **M3-SL**, **M3-PL** and **M3-TR** (table 3, fig.  
322 3). The number of PCs explaining at least 90% of the initial shape variation is 10, 8, 5 and 6,  
323 respectively. The shape variation illustrated by PC1 for **M3-FL** concerns the width and length  
324 of the teeth, with a tendency to be more “compact” (i.e. thinner and smaller) (fig. 3D). For **M3-**  
325 **SL**, the main changes occur on the lingual triangles and anterior loop, with an enlargement on  
326 the lingual side (fig. 3E). Similar changes on the posterior loop are also observed on **M3-PL**.  
327 The first PC of **M3-TR** describes the T3/T4 alternation, with a T3 tending to close. As for m1,  
328 the PC1 tends to separate the two genera, with least overlap for the **M3-SL** analysis and the  
329 largest overlap for the **M3-TR** for which no separation is observed between the two genera (fig.  
330 3G). Again, the two first PCs do not show any clear difference between *Lemmus* species across  
331 all landmark schemes. The M3 tooth lengths follow the same pattern as for m1 with a large  
332 overlap between the two genera. *Lemmus* range from 1.2 to 1.8 mm and *Myopus* from 1.0 to  
333 1.4 mm, with 90% of *M. schisticolor* being included in the *Lemmus* tooth length interval (fig.  
334 3I).

#### 335 4.2. Statistical classification of modern specimens and shape differences

336 Although there was only a relatively small number of individuals from *Myopus* (the smallest  
337 sample), the unbalanced prediction error curves of the landmark schemes do not show particular  
338 bias compared to the balanced ones (fig. 4a). Nonetheless, a bias was noted between the  
339 dimensionality of the predictor (the number of PCs included to build the LDA) and the  
340 prediction error, with an increase when a high number of predictors is used (fig. 4a). This pattern  
341 could be due to the small size of the model samples in relation to the large dimensionality of

342 the shape space, as encountered by Evin et al. (2013). It is likely that with a larger dataset, such  
343 as that presented by Navarro et al. (2018), this pattern would not be observed. The optimal  
344 number of predictors (PCs), *i.e* the one giving the lowest prediction error rate, was selected to  
345 build the discriminant functions of the models and are detailed in table 3. Six models (**m1-FL**,  
346 **m1-SL**, **m1-AL**, **M3-FL**, **M3-SL** and **M3-PL**) have low prediction errors inferior to 5% for  
347 unbalanced samples (the real samples). Models of the m1 tend to have a lower prediction error  
348 compared to those from the M3 (fig. 4b; table 3). Landmark schemes of the m1 taking in account  
349 the anterior loop (**m1-SL** and **m1-AL**) give the best classifications, up to 0.96 and 0.93. The  
350 same pattern is visible on the M3 and the posterior loop, with **M3-SL** having 0.95 optimal  
351 classification score, with **M3-FL** and **M3-PL** having comparable scores of 0.89 and 0.88. In  
352 contrast, the tooth length (**m1-TL** and **M3-TL**) has very low classification scores, with 0.41  
353 and 0.42 respectively, which is comparable to a classification only due to chance.

354 Figure 5 illustrates the shape differences between *Lemmus* and *Myopus* for modern individuals  
355 along the first discriminant axis from the LDA regarding the different landmark schemes. In  
356 terms of the m1 shape, *Myopus* tends to differ from *Lemmus* with: 1) a different orientation of  
357 the lingual triangles, tending to sweep upwards; 2) a simpler anterior loop with a less marked  
358 labial peak; and 3) a LRA3 that extends less deeply over the BRA2 without generating a new  
359 re-entrant angle on the buccal side of the anterior loop. For the M3, *Myopus* tends to differ from  
360 *Lemmus* as follows: 1) an overall stockier tooth; 2) a simpler posterior loop, almost flat; and 3)  
361 a shorter distance between Lm2 and Lm8. For m1 and M3, tooth lengths show a large overlap  
362 with almost all *Myopus* plotting with the smaller *Lemmus* specimens.

#### 363 4.3. Fossil identifications

364 The best performing model (**m1-SL**) obtained with modern specimens allows the identification  
365 of at least one *Myopus* individual in Grotte des Gorges and one in Gully Cave from the Allerød  
366 interstadial-Younger-Dryas transition level, with posterior probabilities at 0.998 and 0.935,

367 respectively (table 4, figure 6a). For these two individuals, similar attributions to *Myopus* were  
368 obtained with other models (**m1-FL**, **m1-AL**) (see supplementary table A). The **m1-TL** model  
369 (table 4, figure 6b) cannot attribute any individuals as a *Myopus* with significant posterior  
370 probabilities and only 9 individuals are confidently identified as *Lemmus*. Most of the  
371 specimens are undetermined.

372 For the M3 (table 4, figure 6c), one tooth has been attributed to *Myopus* at Gully Cave for the  
373 same level, with the best model (**M3-SL**) giving 0.994 of posterior probability. This attribution  
374 was equally obtained with **M3-FL** and **M3-PL** models. No model suggests the presence of  
375 *Myopus* in the M3 sample from Grotte des Gorges, but only three teeth were analysed. As for  
376 **m1-TL**, the **M3-TL** model cannot attribute any individual to *Myopus* with high posterior  
377 probabilities (figure 6d), and the model is unable to confidently identify a large majority of the  
378 specimens (table 4, figure 6).

## 379 **5. Discussion**

380 *Myopus schisticolor* and *Lemmus sp.* are two lemmings that are currently widespread  
381 throughout north Eurasia. They have two distinct habitat preferences, the first inhabits  
382 exclusively taiga forest, whereas the second prefers an open tundra environment (e.g. Mitchell-  
383 Jones et al., 1999; Niethammer and Krapp, 1982). They both consume mosses, but with variable  
384 seasonal proportions: the diet of *Myopus schisticolor* is restricted only to this vegetation type,  
385 whereas *Lemmus sp.* diversifies its diet during spring and summer with dicots, grasses and  
386 sedges being consumed (e.g. Batzli and Pitelka, 1983; Calandra et al., 2015; Eskelinen, 2002;  
387 Rodger and Lewis, 1986). If distinguishing between these two species is relatively easy at the  
388 present day, due to their distinctive external morphology, they are extremely difficult to identify  
389 with fossil material, on account of their similar tooth morphologies.



## 390 5.1. Molar shape differentiation

391 Despite the similarity in tooth morphology of these two lemming genera, the geometric  
392 morphometric approach used in this paper has been able to describe and quantify intergeneric  
393 shape differentiation of the first lower molar (m1) and the third upper molar (M3) of modern  
394 specimens. Describing the whole shape of the molars with a set of landmarks associated with  
395 semi-landmarks on the anterior loop of m1 or posterior loop of M3 (**m1-SL** and **M3-SL**)  
396 appears to be the best landmark scheme among those tested here for the modern reference  
397 framework. These two landmark schemes have allowed us to separate the two genera with high  
398 statistical probabilities, around 0.95 confidence (table 3).

399 These landmark schemes suggest that the main differences between these two genera relate to  
400 the tooth complexity with the outer loops more developed in *Lemmus* than in *Myopus*. The  
401 anterior loop on the m1 or the posterior loop on the M3 tend to exhibit a supplementary angle,  
402 which is not observed in *Myopus*. For *Myopus*, teeth tend to be stockier and simpler in shape.  
403 This increased complexity of the anterior m1 loop in *Lemmus*, always absent in *Myopus*, and  
404 the organisation of the buccal triangles shifting anteriorly on *Lemmus*, are congruent with the  
405 taxonomic literature (Chaline et al., 1988; Markova et al., 2018; Smirnov et al., 1997;  
406 Ponomarev et al., 2013b). Some of these authors also noted that on the M3, the T3/T4  
407 alternation and asymmetry could be used to distinguish both genera. The morphometrical  
408 approach developed in this paper thus offered the opportunity to evaluate these criteria (M3-  
409 TR). Despite the relevance of these criteria, we demonstrate here that they cannot be used to  
410 clearly differentiate the two genera because of a large overlap in their morphology (figure 3;  
411 table 3).

412 Among the external morphological criteria allowing differentiation between these two genera,  
413 their differences in sizes have been regularly mentioned, with *Myopus* being smaller (Borodin,  
414 2009). This criterion was often applied to fossil material through measurement of the length of

415 the teeth or dental row (e.g. Borodin, 2009; Kowalski, 1977; Rhodes et al., 2018). Nonetheless,  
416 as illustrated in figure 3, there is a high overlap between the two genera in terms of tooth length.  
417 This overlap is mainly observed between *M. schisticolor* and *L. lemmus*, whereas *L. sibiricus*  
418 teeth are taller, with a clear separation from other lemmings (figure 3H, I). Applying the  
419 criterion of size to Western European fossil assemblages with lemmings is therefore likely to  
420 conflate *L. lemmus* and *M. schisticolor*, affirming presence of the former but obscuring the  
421 presence of the latter. In any case, size always has to be used very cautiously on fossil species  
422 because it can be highly variable according to the time period, the climate or even the latitude  
423 and altitude (e.g. Delpech, 1999; Klein, 1986, Klein and Scott, 1989).

424 By its ability to capture the whole geometry of an object, geometric morphometrics has  
425 therefore become increasingly popular in archaeological and palaeontological studies (e.g.  
426 Cucchi et al., 2014; Escudé et al., 2008; Evin et al., 2013; Killick., 2012; Marr, 2016; McGuire,  
427 2011; Miele et al., 2020; Navarro et al., 2018). Associated with classification analysis, such as  
428 a LDA, it is a powerful approach that allows differentiation of morphologically close species,  
429 thereby assisting in the robust identification of fossil remains and in our understanding of  
430 changing faunal communities.

## 431 5.2. *Myopus* fossil identifications: palaeobiogeographical implications

432 During Late Pleistocene glaciations, cold environmental conditions were favourable to  
433 lemmings and facilitated their dispersal throughout a large part of Europe (Markova et al., 2019;  
434 Royer, 2013), from the Urals (Ponomarev et. al., 2013) to Ireland (Monaghan, 2017; Sutcliffe  
435 and Kowalski, 1976; Woodman et al., 1996), including for example France (Marquet, 1993;  
436 Royer et al., 2016), Denmark (Bennike et al., 1994; Larsen and Mangerud, 1990) or  
437 Czechoslovakia (Horacek and Sanchez-Marco, 1984). Until the present paper, the presence of  
438 *Myopus* in Western Europe was either not envisaged at all or, at best, still questioned. Our  
439 results attest its presence in two sites from two distinct periods of Late Pleistocene: la Grotte

440 des Gorges, located in East of France, which is from the end of MIS 3, around 30 ka cal BP,  
441 and Gully Cave, situated in the Somerset (England), from the Allerød interstadial - Younger  
442 Dryas transition level.

443 Occurrences of *M. schisticolor* have already been suggested for European Early and Middle  
444 Pleistocene site at Boxgrove (England, Roberts and Parfitt, 1999) and Vergranne (France,  
445 Chaline et al., 1989) and suspicions of its presence (records of *Myopus/Lemmus*) have raised in  
446 Chlum-4 (Czech Republic, Kowalski, 2001), Nyaravai-2 (Lithuania, Kowalski, 2001), and  
447 Sudmer-Berg 2 (Germany, von Koenigswald, 1972). In general, these suspicions are based on  
448 both the morphology of the teeth and on the faunal associations, which are characteristic of a  
449 forest environment. However, these tentative suggestions were not uniformly accepted (van  
450 Kolfschoten, 1995; 1996; Kowalski, 1995, 2001); for example at Vergranne, Kowalski (1995)  
451 stated that the *Myopus* identification cannot be accepted as definitive. His opinion was that it is  
452 not possible to separate *Lemmus* and *Myopus* in the fossil record, and that *Myopus* did not reach  
453 Europe during Pleistocene (Kowalski, 2001). Approaches as geometric morphometrics or  
454 ancient DNA, which provide reliable identification, imply reconsidering certain determinations  
455 based on presuppositions of past studies (geographical area, morphological features, faunal  
456 assemblages). The same issues were recently underlined for other species as for example *Sorex*,  
457 with the identification of the boreal *Sorex tundrensis* in Germany during the end of MIS3  
458 (Freund, 1998; Prost et al., 2013), a species that was not supposed to reach Europe.

459 Lemming specimens from older Early and Middle Pleistocene sites are generally assigned to  
460 ancestral forms of *Lemmus*, possibly *Lemmus kowalskii*. This extinct species is then assumed  
461 to have lived under temperate conditions in a more wooded environment, as suggested by the  
462 forest taxa with which it was associated (van Kolfschoten, 1995; 1996; Kowalski, 1995; 2001).  
463 However, identification of *Lemmus kowalskii* is highly controversial, since it is  
464 morphologically similar to *Myopus*, but much closer in size to *Lemmus* (Harrison *et al.*, 1989).

465 For the Late Pleistocene, several studies attest the presence of *Myopus* in the Ural (Ponomarev  
466 et al., 2013a, b, c) by using the ratios of Smirnov *et al.* (1997) or morphotype differentiation  
467 associated with non-metric multidimensional scaling (Ponomarev et al., 2013a, c). In Europe,  
468 *Lemmus* / *Myopus* remains from this period are always identified as *Lemmus* (*Lemmus lemmus*  
469 in the western part of Europe and *Lemmus sibiricus* in the eastern part). To our knowledge, only  
470 one previous occurrence of *Myopus schisticolor* has been suggested for this period in western  
471 part of Europe, in Level 4 of King Arthur's Cave (Wye Valley, England) (Price, 2003), which  
472 has been attributed to the Bølling-Allerød interstadial (Bronk Ramsey, 2002). Nevertheless,  
473 these determinations (obtained on 12 teeth from a total sample of 17) were only based on tooth  
474 length (Price, 2003) and were not corroborated by another approach, although the presence of  
475 boreal species in the same level, such as *Clethrionomys rufocanus*, tends to strengthen this  
476 hypothesis (Price, 2003). The identification of *Myopus* in the Allerød - interstadial layer of  
477 Gully Cave corroborates Price's suppositions, suggesting the presence of this species during  
478 milder climatic phases in the southern part of England. This presence throughout the  
479 septentrional region of Western Europe (i.e. latitude > 45°N) during the Late Pleistocene, raises  
480 the question of whether its occurrence was (semi)continuous, or sporadic related to specific  
481 climatic events favouring its expansion from eastern regions.

### 482 5.3. Palaeoenvironmental implications of *Myopus* occurrence in Late Pleistocene

483 Since *Myopus* is today closely linked to the taiga, its identification has strong implications for  
484 palaeoenvironmental reconstructions, suggesting past local environments with boreal forest  
485 cover mainly composed of *Pinus*, *Betula* and *Picea*, which is favourable to the development of  
486 the thick moss cover that constitutes nearly all of its diet (Bobretsov and Lukyanova, 2017;  
487 Eskelinen, 2002). Our results from both sites (Grotte des Gorges and Gully Cave) suggest the  
488 association of individuals from both genera *Lemmus* and *Myopus*. While this might appear  
489 contradictory due to their distinct environmental preferences, they were found within a

490 diversified faunal association, including for instance *Dicrostonyx torquatus*, *Alexandromys*  
491 *oeconomus* or *Lasiopodomys gregalis*. Although these fossil faunal communities are  
492 'disharmonious' by comparison to present-day small mammal associations and might therefore  
493 reflect a palimpsest of distinct phases, the stratigraphical integrity of our study samples is clear.  
494 It is therefore more likely that these diverse assemblages reflect the mosaic environment of  
495 boreal forest and steppes that are increasingly recognised as typical of the Late Pleistocene of  
496 northern Europe.

497 Multi-proxy investigations on sediment archives have demonstrated continental vegetation to  
498 be highly sensitive to Dansgaard-Oeschger events (Fletcher et al., 2010), consequently  
499 impacting small mammal communities. Pollen from the Bergsee lacustrine record in Germany  
500 demonstrates a high frequency succession of steppe and boreal forest phases, consistent with  
501 stadial-interstadial oscillations, and underpinned by increases in *Juniperus* and *Pinus* pollen  
502 during Greenland Interstadials 8 and 7 (Becker et al., 2006; Duprat-Oualid et al., 2017). The  
503 presence of *Myopus* in la Grotte des Gorges could therefore be related to one of these Greenland  
504 Interstadial events.

505 For Gully Cave, two levels have been investigated, one attributed to the Allerød interstadial -  
506 Younger Dryas transition, and one from the Younger Dryas. Among individuals from the older  
507 level, at least two teeth suggest the presence of *M. schisticolor* according to the most efficient  
508 models (**m1-SL**: 1, **M3-SL**: 1), but for the cold-climate level of Younger Dryas, no specimens  
509 have been attributed to *M. schisticolor*. Vegetation in Britain was highly sensitive through Late  
510 Glacial stadials and interstadials, with regional variation depending of the latitude (e.g. Birks  
511 and Birks, 2014; Huntley and Birks, 1983; Jones and Keen, 2012; Pennington, 1977; Walker et  
512 al., 2003). In southern England, the Allerød interstadial was a temperate-climate phase  
513 characterized by an increase in forest taxa (Hill et al., 2007; Walker et al., 2003), in particular  
514 the spread of *Betula* (Birks and Birks, 2014). The development of this semi-open boreal

515 environment in southwestern England (Hills et al., 2007) is echoed by the apparent  
516 disappearance of *Equus ferus* at this time (Kaagan, 2000), and favoured the coexistence of both  
517 arctic and boreal species, such as *Cervus elaphus* and *Rangifer tarandus* in Cheddar Gorge  
518 (Carrant and Jacobi, 2011). King Arthur's Cave, which is located 80 km north of Gully Cave,  
519 has equally yielded both forested and cold-adapted taxa (e.g. *Dicrostonyx torquatus*,  
520 *Alexandromys oeconomicus*, *Lasiopodomys gregalis*, *Clethrionomys rufocanus*, *Microtus*  
521 *agrestis*, *Lemmus lemmus*; Price, 2003), suggesting a mosaic environment. This environment  
522 was able to support both *Lemmus* and *Myopus* populations during the Allerød interstadial, with  
523 the presence of both open and forested areas. The abruptness of the succeeding Younger Dryas  
524 cooling event led to drastic vegetation changes, with a decline in forested environments, a  
525 decrease in *Betula*, and a rise of *Artemisia* in southern England (Birks and Birks, 2014).  
526 European *Betula* macrofossils from this period only belong to *Betula nana* (Birks and Birks,  
527 2014), reflecting the reduction of forest and inhibiting the development of the moss cover  
528 needed by *Myopus*.

## 529 **6. Conclusion**

530 Our results highlight that: i) the presence of *Myopus schisticolor* is confirmed for the first time  
531 in the Late Pleistocene fossil record of western Europe, although it remains to be established  
532 whether its occurrence was (semi)continuous or sporadic, only related to specific climatic  
533 events favouring its expansion from eastern regions; ii) its presence has important consequences  
534 for palaeoenvironmental interpretations, implying the existence of boreal open/semi open  
535 environments.

## 536 **Author contributions**

537 Conceptualization, L.A., S.M. and A.R.; Methodology and Software, L.A. and R.L.; Formal  
538 analysis, Investigations and Data Curation, L.A.; Validation: R.L.; Resources, S.M., D.S. and

539 S.D.; Writing original draft preparation and Visualisation, L.A., S.M. and A.R.; Writing,  
540 Review and Editing, L.A., S.M., A.R., D.S., R.L. and S.D.

#### 541 **Acknowledgments**

542 This study was partially supported by the project HARCGLOB (AAP 2020 Région Bourgogne  
543 Franche-Comté). The authors thank Olivier Gilg for giving access to specimens from Victoria  
544 Island. We also thank Jérôme Thomas and ReColNat for giving access to the lemming  
545 specimens housed at Biogeosciences Palaeontology collection, as well as Aleksandr Sokolov  
546 and Natalia Sokolova of the Ural branch of Russian Science Academy for their loan of Siberian  
547 lemming's specimens. Danielle Schreve acknowledges the support of the National Trust and  
548 Natural England in the excavation of Gully Cave.

#### 549 **Figure captions**

550 Figure 1: Landmark schemes (in grey squares) defined for Lemmini first lower molar (m1) and  
551 third upper molar (M3). Hand-placed landmarks are in white, automatically detected landmarks  
552 are in black, and semi-landmarks are in blue (for **m1-SL**, **m1-AL**, **M3-SL** and **M3-AL**) and in  
553 yellow (for **M3-TR**). Abbreviations: T = triangles, LRA = lingual re-entrant angles, BRA =  
554 buccal re-entrant angles, AL = anterior loop, PL = posterior loop. Modified after van der Meulen  
555 (1973).

556

557 Figure 2: A) Global climate evolution and chronology of the last part of the last glacial  
558 following the NGRIP-ice record (Andersen et al., 2004) with the position of the two fossil sites.  
559 Abbreviations: MIS: marine isotope stage, HE: Heinrich events, LGM: last glacial maximum,  
560 BA: Bølling - Allerød interstadial, YD: Younger-Dryas. B) Geographical range of *Lemmus*  
561 *lemmus* (blue), *Lemmus sibiricus* (red) and *Myopus schisticolor* (yellow) with the overlap area  
562 (orange). Circles indicate the location of the modern samples and squares (brown) the  
563 localisation of the fossil samples. Site number: 1. Karigasniemi, 2. Kilpisjärvi, 3. Pällasjarvi-  
564 Muonio, 4. Rovaniemi, 5. Sabetta, 6. Erkuta, 7. Bely Island, 10. Sotkamo area, 11. Posio, 12.  
565 Grotte des Gorges, 13. Gully Cave. Localities from North America and Eastern Siberia are not  
566 shown (see text for detail).

567

568 Figure 3: Morphospaces (PC1 – PC2 planes) of modern specimens with associated shape  
569 variation for all landmark schemes (A: m1-FL; B: m1-SL; C: m1-AL; D: M3-FL; E: M3-SL;  
570 F: M3-PL) and violin plots for tooth length (H: m1-TL; I: M3-TL). For PCA, displayed shape  
571 variation corresponds to morphological changes along the 1st PC axis, depicted by lollipop  
572 graphs (grey outline and black dots for the mean shape, black segments for the shape deviation  
573 from the mean shape to the most distant individual score on the considered PC). Percentage of  
574 shape variation explained by each PC are reported. *Myopus* are in yellow, *Lemmus lemmus* in  
575 blue, *Lemmus sibiricus* in red and *Lemmus trimucronatus* in cyan.

576

577 Figure 4: A) Variation of the LDA's prediction error according to the number of PCs included  
578 to build the model for each landmark scheme, with m1 on the left and M3 on the right. For each  
579 plot, continuous coloured lines show the prediction error for the original samples, dotted  
580 coloured lines show the prediction error for the set of 100 balanced samples, and the grey line  
581 show the prediction error for the set of 100 randomly reassigned samples with the associated  
582 error bars standing for the 95% confidence intervals (null hypothesis). B) Model prediction  
583 error with the optimal number of PCs for each landmark scheme. Coloured points correspond  
584 to the observed prediction error on the real datasets, black points correspond to the prediction  
585 error for the set of 100 balanced samples with the associated 95% confidence interval, grey  
586 points show the prediction error for the set of 100 randomly reassigned samples with the  
587 associated error bars standing for the 95% confidence interval (null hypothesis).

588 Figure 5: Distribution histograms of the modern samples along the linear discriminant axis with  
589 associated shape changes. *Lemmus* are in blue, *Myopus* are in yellow. The displayed shapes  
590 correspond to the extreme individual scores on the discriminant axis for each landmark scheme.

591 Figure 6: Distribution histograms of the fossil samples along the discriminant axis from the  
592 model based on modern samples for m1-SL, m1-TL, M3-SL and M3-TL datasets. Fossil  
593 samples are reported by archaeological/palaeontological levels (scatter plot). *Lemmus* are in  
594 blue, *Myopus* are in yellow.



595 **Table captions**

596 Table 1: List of the analysed specimens with their origin and counts (neighbour localities are  
597 merged). See figure 1 for localities.

598 Table 2: Datasets used in the present study. FL = Fixed landmarks, SL= Semi landmarks  
599 (including FL and AL for m1 and FL and PL for M3), PL = Posterior loop, AL = Anterior loop,  
600 TL = ToothLength.

601 Table 3: Abbreviations: Tot. PCSs= Total Number of PCs, Opt. PCs = Optimal Number of PCs  
602 used in the model, PC1+PC2 = cumulative proportion of variance explained by PC1 + PC2, %  
603 Opt. class. actual = percentage of prediction error of modern specimens with the optimal  
604 number of PCs.

605 Table 4: Fossil identification for m1 and M3. The number of specimens identified with  
606 associated posterior probabilities > 0.9 are in brackets

607 Supplementary data captions

608 Supplementary table 1: classification of fossil specimens for each dataset with associated  
609 posterior probabilities for m1 and M3.

610 **Data availability statement**

611 All data and codes are available on request from the authors.

612 **References**

613 Abramson, N.I., 1993. Evolutionary trends in the dentition of true lemmings (Lemmini,  
614 Cricetidae, Rodentia): functional-adaptive analysis. *Journal of Zoology* 230, 687–699.  
615 <https://doi.org/10.1111/j.1469-7998.1993.tb02717.x>

616 Abramson, N.I., Nadachowski, A., 2001. Revision of lemmings (Lemminae) from Poland with  
617 special reference of the occurrence of *Synaptomys* in Eurasia. *Acta zoologica cracoviensia*,  
618 44(1), 65-77. <https://doi.org/10.1111/j.1469-7998.1993.tb02717.x>

619 Abramson, N.I., Petrova, T.V., 2018. Genetic analysis of type material of the Amur lemming  
620 resolves nomenclature issues and creates challenges for the taxonomy of true lemmings  
621 (Lemmus, Rodentia: Cricetidae) in the eastern Palearctic. *Zoological Journal of the*  
622 *Linnean Society* 182, 465–477. <https://doi.org/10.1093/zoolinnea/zlx044>

- 623 Andersen, K.K., Azuma, N., Barnola, J.M., Bigler, M. et al., 2004. High-resolution record of  
624 Northern Hemisphere climate extending into the last interglacial period. *Nature*, 2004. v.  
625 431, No. 7005. 147–151.
- 626 Batzli, G.O., Pitelka, F.A., 1983. Nutritional Ecology of Microtine Rodents: Food Habits of  
627 Lemmings near Barrow, Alaska. *Journal of Mammalogy* 64, 648–655.  
628 <https://doi.org/10.2307/1380521>
- 629 Baylac, M., Frieß, M., 2005. Fourier Descriptors, Procrustes Superimposition, and Data  
630 Dimensionality: An Example of Cranial Shape Analysis in Modern Human Populations,  
631 in: Slice, D.E. (Ed.), *Modern Morphometrics in Physical Anthropology, Developments in*  
632 *Primateology: Progress and Prospects*. Kluwer Academic Publishers-Plenum Publishers,  
633 New York, pp. 145–165. [https://doi.org/10.1007/0-387-27614-9\\_6](https://doi.org/10.1007/0-387-27614-9_6)
- 634 Becker, A., Ammann, B., Anselmetti, F., Marie Hirt, A., Magny, M., Millet, L., Rachoud, A.-  
635 M., Sampietro, G., Wüthrich, C., 2006. Paleoenvironmental studies on lake Bergsee, Black  
636 Forest, Germany. *Neues Jahrbuch für Geologie und Paläontologie* 240, 405–445.
- 637 Bennike, O., Houmark-Nielsen, M., Böcher, J., Heiberg, E.O., 1994. A multi-disciplinary  
638 macrofossil study of Middle Weichselian sediments at Kobbeltgård, Møn, Denmark.  
639 *Palaeogeography, Palaeoclimatology, Palaeoecology* 111, 1–15.  
640 [https://doi.org/10.1016/0031-0182\(94\)90344-1](https://doi.org/10.1016/0031-0182(94)90344-1)
- 641 Birks, H.H., Birks, H.J.B., 2014. To what extent did changes in July temperature influence  
642 Lateglacial vegetation patterns in NW Europe? *Quaternary Science Reviews* 106, 262–  
643 277. <https://doi.org/10.1016/j.quascirev.2014.06.024>
- 644 Bobretsov, A.V., Lukyanova, L.E., 2017. Population dynamics of wood lemming (*Myopus*  
645 *schisticolor*) in different landscapes of the Northern Pre-Urals. *Rus.J.Theriol.* 16, 86–93.  
646 <https://doi.org/10.15298/rusjtheriol.16.1.08>
- 647 Bookstein, F.L., 1997. *Morphometric Tools for Landmark Data: Geometry and Biology*.  
648 Cambridge University Press.
- 649 Borodin, A.V., 2009. *A Diagnostic Guide to Teeth of Arvicolines of the Urals and Western*  
650 *Siberia, from the Late Pleistocene to the Present*. Ural Branch of the Russian Academy of  
651 Sciences Publishing, Yekaterinburg, 100 pp. (in Russian).

- 652 Buzan, E.V., Krystufek, B., Hänfling, B., Hutchinson, W.F., 2008. Mitochondrial phylogeny of  
653 Arvicolinae using comprehensive taxonomic sampling yields new insights: Phylogeny of  
654 Arvicolinae. *Biological Journal of the Linnean Society* 94, 825–835.  
655 <https://doi.org/10.1111/j.1095-8312.2008.01024.x>
- 656 Calandra, I., Labonne, G., Mathieu, O., Henttonen, H., Lévêque, J., Milloux, M.-J., Renvoisé,  
657 É., Montuire, S., Navarro, N., 2015. Isotopic partitioning by small mammals in the  
658 subnivium. *Ecol Evol* 5, 4132–4140. <https://doi.org/10.1002/ece3.1653>
- 659 Chaline, J., Brunet-Lecomte, P., Brochet, G., Martin, F., 1989. Les lemmings fossiles du genre  
660 Lemmus (Arvicolidae, Rodentia) dans le pléistocène de France. *Geobios* 22, 613–623.  
661 [https://doi.org/10.1016/S0016-6995\(89\)80115-9](https://doi.org/10.1016/S0016-6995(89)80115-9)
- 662 Chaline, J., Brunet-Lecomte, P., Kaikusalo, A., Martin, F., Brochet, G., 1988. Discrimination  
663 de la morphologie dentaire de Lemmus lemmus et Myopus schisticolor (Arvicolidae,  
664 Rodentia) par l'analyse multivariée. *Mammalia* 52, 259–274.  
665 <https://doi.org/10.1515/mamm.1988.52.2.259>
- 666 Chaline, J., 1972. Les rongeurs du Pléistocène moyen et supérieur de France. *Cahiers de*  
667 *Paléontologie*, éd du CNRS, Paris, 410
- 668 Chaline, J., Mein, P., 1979, *Les rongeurs et l'évolution*. Doin, Paris, 235
- 669 Cheprakov, M.I., 2016. Встречаемость отложений цемента в терминальных синклиналиях  
670 моляров у евразийских представителей трибы Lemmini (Rodentia, Arvicolinae). *Зоол.*  
671 *ж.* 95, 966–975. <https://doi.org/10.7868/S0044513416060076>
- 672 Cook, J.A., Runck, A.M., Conroy, C.J., 2004. Historical biogeography at the crossroads of the  
673 northern continents: molecular phylogenetics of red-backed voles (Rodentia: Arvicolinae).  
674 *Molecular Phylogenetics and Evolution* 30, 767–777. [https://doi.org/10.1016/S1055-](https://doi.org/10.1016/S1055-7903(03)00248-3)  
675 [7903\(03\)00248-3](https://doi.org/10.1016/S1055-7903(03)00248-3)
- 676 Cox, P.G., Hautier, L., 2015. *Evolution of the Rodents: Advances in Phylogeny, Functional*  
677 *Morphology and Development*. Cambridge University Press.
- 678 Cucchi, T., Barnett, R., Martínková, N., Renaud, S., Renvoisé, E., Evin, A., Sheridan, A.,  
679 Mainland, I., Wickham-Jones, C., Tougaard, C., Quéré, J.P., Pascal, Michel, Pascal, Marine,  
680 Heckel, G., O'Higgins, P., Searle, J.B., Dobney, K.M., 2014. The changing pace of insular

681 life: 5000 years of microevolution in the orkney vole (*Microtus arvalis orcadensis*).  
682 Evolution 68, 2804–2820. <https://doi.org/10.1111/evo.12476>

683 Currant, A.P., Jacobi, R., 2011. The Mammal Faunas of the British Late Pleistocene, in:  
684 Developments in Quaternary Sciences. Elsevier, pp. 165–180.  
685 <https://doi.org/10.1016/B978-0-444-53597-9.00010-8>

686 David, S., d’Errico, F., Pigeaud, R., Bereizat, G., Robert, E., Cailhol, D., Petrognani, S., Griggo,  
687 C., Jaillet, S., Jeannet, M., Paitiere, H., 2014. La grotte des Gorges ( Jura ) : un site inédit à  
688 l’interface des territoires symboliques du Paléolithique supérieur ancien., in: Ricalens,  
689 M.O.& F.L.B. (Ed.), Modes de Contacts et de Déplacements Au Paléolithique  
690 Eurasiatique.

691 David, S., Pigeaud, R., Battesti, D., Cailhol, D., Corbé, M., Ferrier, C., Paitier, H., Tirologos,  
692 G., Vuillermoz, D., 2017. L’art mobilier de la grotte des Gorges (Amange, Jura, France).  
693 Approche méthodologique et premiers résultats. in Cleyet-Merle J.-J., Geneste J.-M., Man-  
694 Estier E. (dir.), L’art au quotidien - Objets ornés du Paléolithique supérieur. Actes du  
695 colloque international, Les Eyzies-de-Tayac, 16-20 juin 2014 PALEO, numéro spécial.

696 Delpech F., 1999. Biomasse d’Ongulés au Paléolithique et inférences sur la démographie. Paléo,  
697 11, 19-42

698 Domine, F., Gauthier, G., Vionnet, V., Fauteux, D., Dumont, M., Barrere, M., 2018. Snow  
699 physical properties may be a significant determinant of lemming population dynamics in  
700 the high Arctic. Arctic Science 4, 813–826. <https://doi.org/10.1139/as-2018-0008>

701 Dryden, I.L. and Mardia, K.V., 1998. Statistical shape analysis, John Wiley and Sons,  
702 Chichester.

703 Duprat-Oualid, F., Rius, D., Bégeot, C., Magny, M., Millet, L., Wulf, S., Appelt, O., 2017.  
704 Vegetation response to abrupt climate changes in Western Europe from 45 to 14.7k cal a  
705 BP: the Bergsee lacustrine record (Black Forest, Germany). Journal of Quaternary Science  
706 32, 1008–1021. <https://doi.org/10.1002/jqs.2972>

707 Escudé, E., Montuire, S., Desclaux, E., Quéré, J.-P., Renvoisé, E., Jeannet, M., 2008.  
708 Reappraisal of ‘chronospecies’ and the use of *Arvicola* (Rodentia, Mammalia) for  
709 biochronology. Journal of Archaeological Science 35, 1867–1879.  
710 <https://doi.org/10.1016/j.jas.2007.11.018>

- 711 Eskelinen, O., 2002 Diet of the wood lemming *Myopus schisticolor*. *Annales Zoologici Fennici*  
712 vol. 39: 49-57.
- 713 Evin, A., Cucchi, T., Cardini, A., Strand Vidarsdottir, U., Larson, G., Dobney, K., 2013. The  
714 long and winding road: identifying pig domestication through molar size and shape.  
715 *Journal of Archaeological Science* 40, 735–743. <https://doi.org/10.1016/j.jas.2012.08.005>
- 716 Fejfar, O., Heinrich, W.-D., 1989. Muroid Rodent Biochronology of the Neogene and  
717 Quaternary in Europe, in: Lindsay, E.H., Fahlbusch, V., Mein, P. (Eds.), *European*  
718 *Neogene Mammal Chronology*, NATO ASI Series. Springer US, Boston, MA, pp. 91–117.  
719 [https://doi.org/10.1007/978-1-4899-2513-8\\_7](https://doi.org/10.1007/978-1-4899-2513-8_7)
- 720 Fletcher, W.J., Sánchez Goñi, M.F., Allen, J.R.M., Cheddadi, R., Combourieu-Nebout, N.,  
721 Huntley, B., Lawson, I., Londeix, L., Magri, D., Margari, V., Müller, U.C., Naughton, F.,  
722 Novenko, E., Roucoux, K., Tzedakis, P.C., 2010. Millennial-scale variability during the  
723 last glacial in vegetation records from Europe. *Quaternary Science Reviews* 29, 2839–  
724 2864. <https://doi.org/10.1016/j.quascirev.2009.11.015>
- 725 Freund D, 1998. *Sesselfelsgrötte I: Grabungsverlauf und Stratigraphie.*, Saarbrücken,  
726 Saarbrücker Dr. und Verl.
- 727 Gobalet, K.W., 2001. A Critique of Faunal Analysis; Inconsistency among Experts in Blind  
728 Tests. *Journal of Archaeological Science* 28, 377–386.  
729 <https://doi.org/10.1006/jasc.2000.0564>
- 730 Gromov, I.M., Polyakov, I.Y., 1992. Voles (Microtinae). *Fauna of the USSR, mammals*, Vol.  
731 3, No 8.
- 732 Harrison, D.L., Bates, P.J.J., Clayden, J.D., 1989. Occurrence of *Lemmus kowalskii* Carls and  
733 Rabeder, 1988 (Rodentia: Microtinae: *Lemmus*) in the Lower Pleistocene of East Anglia.  
734 *Acta Theriol.* 34, 55–65. <https://doi.org/10.4098/AT.arch.89-3>
- 735 Hernández Fernández, M., 2006. Rodent paleofaunas as indicators of climatic change in Europe  
736 during the last 125,000 years. *Quat. res.* 65, 308–323.  
737 <https://doi.org/10.1016/j.yqres.2005.08.022>
- 738 Hill, T.C.B., Woodland, W.A., Spencer, C.D., Marriott, S.B., Case, D.J., Catt, J.A., 2008.  
739 Devensian Late-glacial environmental change in the Gordano Valley, North Somerset,

740 England: a rare archive for southwest Britain. *J Paleolimnol* 40, 431–444.  
741 <https://doi.org/10.1007/s10933-007-9171-5>

742 Horáček, I., Sánchez Marco, A., 1984. Comments on the Weichselian small mammal  
743 assemblages in Czechoslovakia and their stratigraphical interpretation. *N. Jb. Geol.*  
744 *Paläont. Mh.*, 1984(9), 560–576. <https://doi.org/10.1127/njgpm/1984/1984/560>

745 Hulme-Beaman, Ardern, Cucchi, T., Evin, A., Searle, J.B., Dobney, K., 2018. Exploring *Rattus*  
746 *praetor* (Rodentia, Muridae) as a possible species complex using geometric morphometrics  
747 on dental morphology. *Mammalian Biology* 92, 62–67.  
748 <https://doi.org/10.1016/j.mambio.2018.04.002>

749 Huntley, B., Birks, H.J.B. 1983. An atlas of past and present pollen maps for Europe, 0-13,000  
750 years ago. Cambridge University Press, 667

751 Jones, R.L., Keen, D.H., 2012. Pleistocene Environments in the British Isles. Springer Science  
752 & Business Media, 368

753 Kaagan, L.M., 2000. The horse in late Pleistocene and Holocene Britain (Doctoral). Doctoral  
754 thesis, University of London. University of London, 432

755 Killick, L., 2012. Geometric Morphometric analysis of the *Microtus* M1 and its application to  
756 Early Middle Pleistocene in the UK. (Doctoral). Durham University, 393

757 Klein R.G., 1986. Carnivore size and quaternary climatic change in southern Africa. *Quaternary*  
758 *Research*, 26(1), 153-170

759 Klein R.G., Scott K., 1989. Glacial/interglacial size variation in fossil spotted hyenas (*Crocuta*  
760 *crocuta*) from Britain. *Quaternary Research*, 32(1), 88-95

761 Koenigswald, W., V., 1972. Sudmer-Berg-2, a fauna of the early middle Pleistocene from the  
762 Harz. *Neues Jahrbuch für Geologie und Paläontologie Abhandlungen*, vol. 141, p. 194-221.

763 Koenigswald, W., V., Martin, L., D., 1984. Revision of the fossil and recent Lemninae  
764 (Rodentia, Mammalia). *Papers in Vertebrate Paleontology honoring Robert Warren*  
765 *Wilson*. Carnegie Museum of Natural History Special Publication, 9, 122-137

766 Kolendrianou, M., Ligkovanlis, S., Maniakas, I., Tzortzi, M., Iliopoulos, G., 2020. The  
767 Palaeolithic cave of Kalamakia (Mani Peninsula), Greece: new insights on the

768 palaeoenvironment using microvertebrates and mesowear analysis of ruminant teeth.  
769 Heliyon 6, e03958. <https://doi.org/10.1016/j.heliyon.2020.e03958>

770 Kolfschoten, T.V., 1995. On the application of fossil mammals to the reconstruction of the  
771 palaeoenvironment of northwestern Europe. *Acta zool. cracov.* 38(1): 73-84

772 Kolfschoten, T.V., 1996. Mammalian remains in a Palaeolithic context. *Archaeology,*  
773 *Methodology and the Organisation of Research.* ABACO Edizioni, Forlì, 19-35.

774 Kovarovic, K., Aiello, L.C., Cardini, A., Lockwood, C.A., 2011. Discriminant function  
775 analyses in archaeology: are classification rates too good to be true? *Journal of*  
776 *Archaeological Science* 38, 3006–3018. <https://doi.org/10.1016/j.jas.2011.06.028>

777 Kowalski, K., 1977. Fossil lemmings [Mammalia, Rodentia] from the Pliocene and early  
778 Pleistocene of Poland. *Acta zool. cracov.* 22(7): 297-318

779 Kowalski, K., 1995. Lemmings [Mammalia, Rodentia] as indicators of temperature and  
780 humidity in the European Quaternary. *Acta zool. cracov.* 38(1): 85-94

781 Kowalski, K., 2001. Pleistocene rodents of Europe. *Folia Quaternaria* 72: 3–389.

782 Larsen, E., Mangerud, J., 1989. Marine caves: On-off signals for glaciations. *Quaternary*  
783 *International* 3–4, 13–19. [https://doi.org/10.1016/1040-6182\(89\)90069-4](https://doi.org/10.1016/1040-6182(89)90069-4)

784 Le Vaillant, M., Erlandsson, R., Elmhagen, B., Hörnfeldt, B., Eide, N.E., Angerbjörn, A., 2018.  
785 Spatial distribution in Norwegian lemming *Lemmus lemmus* in relation to the phase of the  
786 cycle. *Polar Biol* 41, 1391–1403. <https://doi.org/10.1007/s00300-018-2293-6>

787 Lyman, R. L., 2002. Taxonomic identification of zooarchaeological remains, *The Review of*  
788 *Archaeology*, 23(2), 13-20

789 Lyman, R.L., 2019. Assumptions and Protocol of the Taxonomic Identification of Faunal  
790 Remains in Zooarchaeology: a North American Perspective. *J Archaeol Method Theory*  
791 26, 1376–1438. <https://doi.org/10.1007/s10816-019-09414-0>

792 Markova, A.K., van Kolfschoten, T., Bohncke, S.J.P., Kosintsev, P.A., Mol, J., Puzachenko,  
793 A.Y., Simakova, A.N., Smirnov, N.G., Verpoorte, A., Golovachev, I.B., 2019. Institute of  
794 geography of Russian Academy of Sciences, 279.

795 Markova, E.A., Bobretsov, A.V., Starikov, V.P., Cheprakov, M.I., Borodin, A.V., 2018.  
796 Unification of Criteria for Distinguishing Morphotypes of Cheek Teeth in Lemmings

797 (Lemmini, Arvicolinae, Rodentia). *Biology Bulletin* 45, 1083–1095.  
798 <https://doi.org/10.1134/S106235901809011X>

799 Marquet, J.-C., Lorblanchet, M., Oberlin, C., Thamo-Bozso, E., Aubry, T., 2016. Nouvelle  
800 datation du « masque » de La Roche-Cotard (Langeais, Indre-et-Loire, France). *Paleo.*  
801 *Revue d'archéologie préhistorique* 253–263. <https://doi.org/10.4000/paleo.3144>

802 Marr, M.M., 2016. Faunal response to abrupt climate change: the history of the British mammal  
803 fauna from the Lateglacial to the Holocene. Doctoral thesis, University of London, 375.

804 van der Meulen, A.J., 1973. Middle Pleistocene smaller mammals from the Monte Pegalia  
805 (Orvieto, Italy) with special reference to the phylogeny of *Microtus* (Arvicolidae,  
806 Rodentia), *Quaternaria*, vol. 17, 1–144.

807 McGuire, J.L., 2011. Identifying California *Microtus* species using geometric morphometrics  
808 documents Quaternary geographic range contractions. *Journal of Mammalogy* 92(6),  
809 1383–1394. <https://doi.org/10.1644/10-MAMM-A-280.1>

810 Miele, V., Dussert, G., Cucchi, T., Renaud, S., 2020. Deep learning for species identification  
811 of modern and fossil rodent molars (preprint). *Zoology*.  
812 <https://doi.org/10.1101/2020.08.20.259176>

813 Mitchell-Jones, A. J., Amori, G., Bogdanowicz, W., Krystufek, B., Reijnders, P. J. H.,  
814 Spitzenberger, F., Stubbe, M., Thissen, J. B. M., Voralik, V., & Zima, J., 1999. The atlas  
815 of European mammals (Vol.3). London: Academic Press.

816 Monaghan, N.T., 2017. Irish Quaternary Vertebrates, in: Coxon, P., McCarron, S., Mitchell, F.  
817 (Eds.), *Advances in Irish Quaternary Studies*. Atlantis Press, Paris, pp. 255–291.  
818 [https://doi.org/10.2991/978-94-6239-219-9\\_9](https://doi.org/10.2991/978-94-6239-219-9_9)

819 Montuire, S., Michaux, J., Legendre, S., Aguilar, J.-P., 1997. Rodents and climate. 1. A model  
820 for estimating past temperatures using arvicolids (Mammalia: Rodentia).  
821 *Palaeogeography, Palaeoclimatology, Palaeoecology* 128, 187–206.  
822 [https://doi.org/10.1016/S0031-0182\(96\)00038-7](https://doi.org/10.1016/S0031-0182(96)00038-7)

823 Montuire, S., Royer, A., Lemanik, A., Gilg, O., Sokolova, N., Sokolov, A., Desclaux, E.,  
824 Nadachowski, A., Navarro, N., 2019. Molar shape differentiation during range expansions  
825 of the collared lemming (*Dicrostonyx torquatus*) related to past climate changes.



- 826 Quaternary Science Reviews 221, 105886.  
827 <https://doi.org/10.1016/j.quascirev.2019.105886>
- 828 Nadachowski, A., 1982. Late quaternary rodents of Poland with special reference to  
829 morphotype dentition analysis of voles. Państwowe Wydawnictwo Naukowe Warszawa,  
830 Kraków. 109
- 831 Navarro, N., Montuire, S., Laffont, R., Steimetz, E., Onofrei, C., Royer, A., 2018. Identifying  
832 Past Remains of Morphologically Similar Vole Species Using Molar Shapes. Quaternary  
833 1, 20. <https://doi.org/10.3390/quat1030020>
- 834 Niethammer, J., & Krapp, F., 1982. Handbuch der Säugetiere Europas. Band 2/I. Nagetiere II.  
835 Wiesbaden (DE): Akademische Verlagsgesellschaft.
- 836 Ognev, S.I., 1948. Mammals of the U.S.S.R and adjacent countries. Rodents. Israel Program  
837 for Scientific Translation, Jerusalem, 6: 354-461.
- 838 Pennington, W., Bertie, D.M., Mitchell, G.F., West, R.G., 1977. The Late Devensian flora and  
839 vegetation of Britain. Philosophical Transactions of the Royal Society of London. B,  
840 Biological Sciences 280, 247–271. <https://doi.org/10.1098/rstb.1977.0109>
- 841 Ponomarev, D., Puzachenko, A., Bachura, O., Kosintsev, P., van der Plicht, J., 2013a. Mammal  
842 fauna during the Late Pleistocene and Holocene in the far northeast of Europe: Late  
843 Pleistocene and Holocene mammal fauna, NE Europe. Boreas 42, 779–797.  
844 <https://doi.org/10.1111/j.1502-3885.2012.00309.x>
- 845 Ponomarev, D., Puzachenko, A., Isaychev, K., 2013b. Morphotypic variability of masticatory  
846 surface pattern of molars in the recent and Pleistocene *Lemmus* and *Myopus* (Rodentia,  
847 Cricetidae) of Europe and Western Siberia. Acta Zoologica 96, 14–29.  
848 <https://doi.org/10.1111/azo.12047>
- 849 Ponomarev, D., van Kolfschoten, T., van der Plicht, J., 2013c. Late Glacial and Holocene small  
850 mammals of the Timan Ridge (Komi Republic, Russia). Quaternary International 284,  
851 177–183. <https://doi.org/10.1016/j.quaint.2012.04.027>
- 852 Price, C.R., 2003. Late Pleistocene and Early Holocene Small Mammals in South West Britain:  
853 Environmental and Taphonomic Implications and Their Role in Archaeological Research.  
854 Archaeopress. British archaeological reports: British series, vol. 347. 115.

- 855 Prost, S., Klietmann, J., van Kolfschoten, T., Guralnick, R.P., Waltari, E., Vrieling, K., Stiller,  
856 M., Nagel, D., Rabeder, G., Hofreiter, M., Sommer, R.S., 2013. Effects of late quaternary  
857 climate change on Palearctic shrews. *Glob Change Biol* 19, 1865–1874.  
858 <https://doi.org/10.1111/gcb.12153>
- 859 Ramsey, C.B., Higham, T.F.G., Owen, D.C., Pike, A.W.G., Hedges, R.E.M., 2002.  
860 Radiocarbon Dates from the Oxford Ams System: *Archaeometry Datelist* 31.  
861 *Archaeometry* 44, 1–150. <https://doi.org/10.1111/j.1475-4754.2002.tb01101.x>
- 862 Reid, D.G., Bilodeau, F., Krebs, C.J., Gauthier, G., Kenney, A.J., Gilbert, B.S., Leung, M.C.-  
863 Y., Duchesne, D., Hofer, E., 2012. Lemming winter habitat choice: a snow-fencing  
864 experiment. *Oecologia* 168, 935–946. <https://doi.org/10.1007/s00442-011-2167-x>
- 865 Reimer PJ, Bard E, Bayliss A, Beck JW, Blackwell PG, Bronk Ramsey C, Buck CE, Cheng H,  
866 Edwards RL, Friedrich M, Grootes PM, Guilderson TP, Haflidason H, Hajdas I, Hatté C,  
867 Heaton TJ, Hoffmann DL, Hogg AG, Hughen KA, Kaiser KF, Kromer B, Manning SW,  
868 Niu M, Reimer RW, Richards DA, Scott EM, Southon JR, Staff RA, Turney CSM, van der  
869 Plicht J. 2013. IntCal13 and Marine13 radiocarbon age calibration curves 0–50,000 years  
870 cal BP. *Radiocarbon* 55(4):1869–1887.
- 871 Rekovets, L.I., Kovalchuk, O.M., 2017. Phenomenon in the Evolution of Voles (Mammalia,  
872 Rodentia, Arvicolidae). *Vestnik Zoologii* 51, 99–110. [https://doi.org/10.1515/vzoo-2017-](https://doi.org/10.1515/vzoo-2017-0015)  
873 [0015](https://doi.org/10.1515/vzoo-2017-0015)
- 874 Rhodes, S.E., Ziegler, R., Starkovich, B.M., Conard, N.J., 2018. Small mammal taxonomy,  
875 taphonomy, and the paleoenvironmental record during the Middle and Upper Paleolithic  
876 at Geißenklösterle Cave (Ach Valley, southwestern Germany). *Quaternary Science*  
877 *Reviews* 185, 199–221. <https://doi.org/10.1016/j.quascirev.2017.12.008>
- 878 Robert, M.B., and Parfitt, S.A., 1999. Boxgrove, a Middle Pleistocene hominid site at Earthan  
879 Quarry, Boxgrove, West Sussex. English Heritage, Archaeological report 17, pp. 339
- 880 Robovský, J., Řičánková, V., Zrzavý, J., 2008. Phylogeny of Arvicolinae (Mammalia,  
881 Cricetidae): utility of morphological and molecular data sets in a recently radiating clade.  
882 *Zoologica Scripta* 37, 571–590. <https://doi.org/10.1111/j.1463-6409.2008.00342.x>
- 883 Rodgers, A.R., Lewis, M.C., 1986. Diet selection in Arctic lemmings ( *Lemmus sibiricus* and  
884 *Dicrostonyx groenlandicus* ): demography, home range, and habitat use. *Canadian Journal*  
885 *of Zoology* 64, 2717–2727. <https://doi.org/10.1139/z86-396>

- 886 Rohlf, F.J., Slice, D., 1990. Extensions of the Procrustes Method for the Optimal  
887 Superimposition of Landmarks. *Systematic Zoology* 39, 40.  
888 <https://doi.org/10.2307/2992207>
- 889 Royer, A., 2013. Etude paléoenvironnementale et paléoclimatique du Pléistocène supérieur du  
890 Sud-Ouest de la France, à partir d'analyses comparées d'associations fauniques et de  
891 biogéochimies effectuées sur les micromammifères. Doctoral Thesis, Ecole Pratique des  
892 Hautes Etudes, 411.
- 893 Royer, A., 2016. How complex is the evolution of small mammal communities during the Late  
894 Glacial in southwest France ? *Quaternary International* 414, 23–33.  
895 <https://doi.org/10.1016/j.quaint.2015.12.065>
- 896 Royer, A., Montuire, S., Legendre, S., Discamps, E., Jeannet, M., Lécuyer, C., 2016.  
897 Investigating the Influence of Climate Changes on Rodent Communities at a Regional-  
898 Scale (MIS 1-3, Southwestern France). *PLOS ONE* 11, e0145600.  
899 <https://doi.org/10.1371/journal.pone.0145600>
- 900 Royer, A., García Yelo, B.A., Laffont, R., Hernández Fernández, M., 2020. New bioclimatic  
901 models for the quaternary palaeartic based on insectivore and rodent communities.  
902 *Palaeogeography, Palaeoclimatology, Palaeoecology* 560, 110040.  
903 <https://doi.org/10.1016/j.palaeo.2020.110040>
- 904 Smirnov, N.G., Golovachev, I.B., Kuznetsova, I.A., Cheprakov, M.I., 1997. Complicated cases  
905 of identifying rodent teeth from Late Pleistocene and Holocene deposits of tundra regions  
906 of Northern Eurasia. In: Kosintsev, P.A. (Ed.), *Materialy Po Istorii I Sovremennomu*  
907 *Sostojaniju Fauny Severa Zapadnoj Sibiri: Sbornik Nauchnyh Trudov*, 60e90. Riphey,  
908 Chelyabinsk (in Russian).
- 909 Stahl, P.W., 1996. The recovery and interpretation of microvertebrate bone assemblages from  
910 archaeological contexts. *J Archaeol Method Theory* 3, 31–75.  
911 <https://doi.org/10.1007/BF02228930>
- 912 Stenseth, N.C., Ims, R.A., 1993. *Biology of lemmings*. Published for the Linnean Society of  
913 London by Academic Press.
- 914 Stoetzel, E., Cornette, R., Lalis, A., Nicolas, V., Cucchi, T., Denys, C., 2017. Systematics and  
915 evolution of the *Meriones shawii/grandis* complex (Rodentia, Gerbillinae) during the Late  
916 Quaternary in northwestern Africa: Exploring the role of environmental and anthropogenic

917 changes. Quaternary Science Reviews 164, 199–216.  
918 <https://doi.org/10.1016/j.quascirev.2017.04.002>

919 Sutcliffe, A.J., Sutcliffe, A.J., Kowalski, K., 1976. Pleistocene rodents of the british isles.  
920 Bulletin of the British Museum (Natural History). 27, 31–147.

921 Tiunov, M.P., Panasenko, V.E., 2011. The distribution history of the Amur brown lemming  
922 (*Lemmus amurensis*) in the Late Pleistocene – Holocene in the southern Far East of Russia.  
923 *Rus.J.Theriol.* 9, 33–37. <https://doi.org/10.15298/rusjtheriol.09.1.05>

924 Walker, M.J.C., Coope, G.R., Sheldrick, C., Turney, C.S.M., Lowe, J.J., Blockley, S.P.E.,  
925 Harkness, D.D., 2003. Devensian Lateglacial environmental changes in Britain: a multi-  
926 proxy environmental record from Llanilid, South Wales, UK. *Quaternary Science Reviews*  
927 22, 475–520. [https://doi.org/10.1016/S0277-3791\(02\)00247-0](https://doi.org/10.1016/S0277-3791(02)00247-0)

928 Wilson, D.E., Lacher, T.E., Mittermeier, R.A. (Eds.), 2017. Handbook of the Mammals of the  
929 World, vol. 7. Lynx Edicions, Barcelona. 1008. Rodent II.

930 Woodman, P., Mccarthy, M., Monaghan, N., 1997. The Irish quaternary fauna project.  
931 *Quaternary Science Reviews* 16, 129–159. [https://doi.org/10.1016/S0277-3791\(96\)00037-](https://doi.org/10.1016/S0277-3791(96)00037-6)  
932 [6](https://doi.org/10.1016/S0277-3791(96)00037-6)

933 Zelditch, M.L., Swiderski, D.L., Sheets, H.D., 2012. Introduction, in: *Geometric*  
934 *Morphometrics for Biologists*. Elsevier, pp. 1–20. [https://doi.org/10.1016/B978-0-12-](https://doi.org/10.1016/B978-0-12-386903-6.00001-0)  
935 [386903-6.00001-0](https://doi.org/10.1016/B978-0-12-386903-6.00001-0)

936

937

938

939

940

941

942

943

944

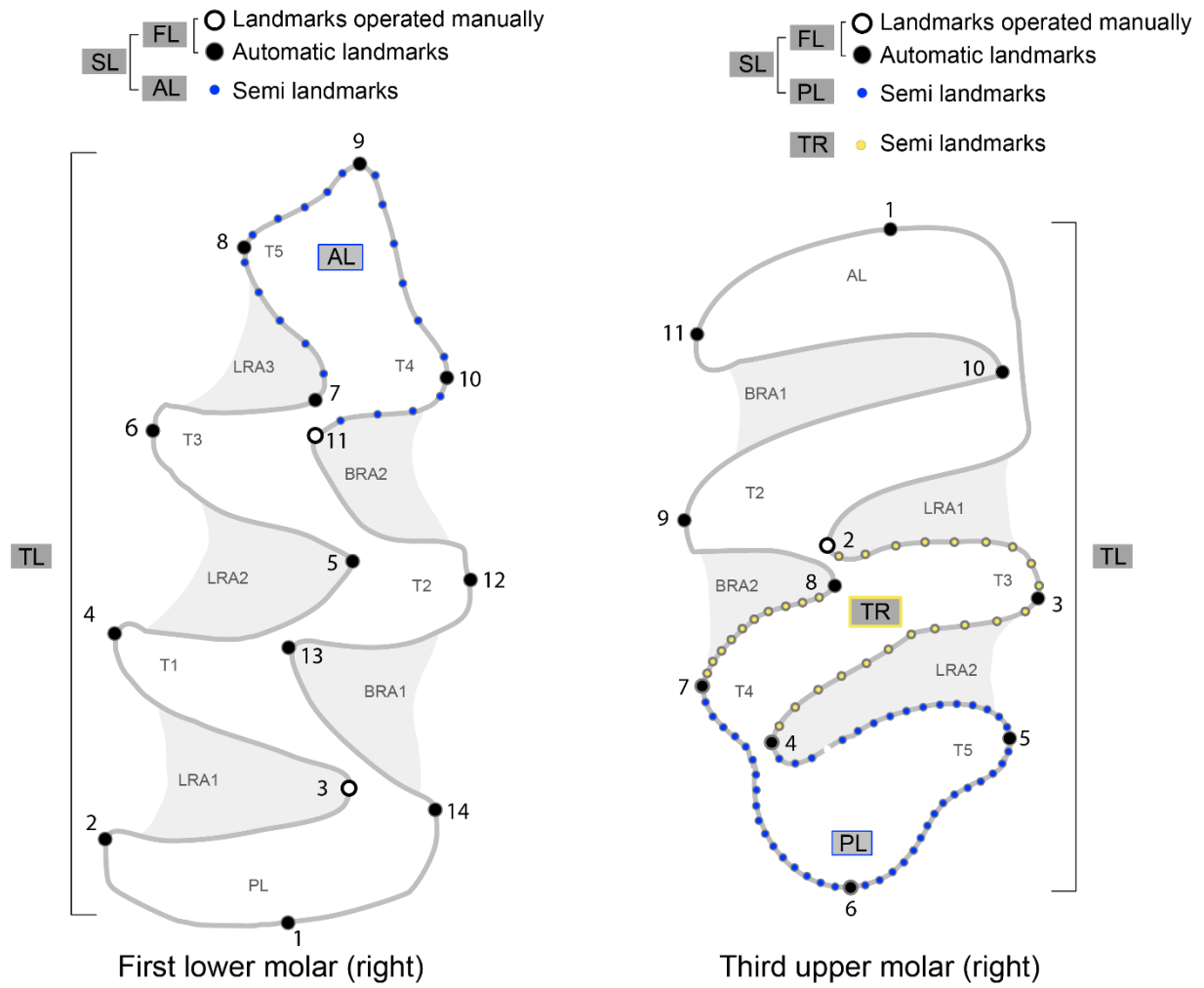


Figure 1

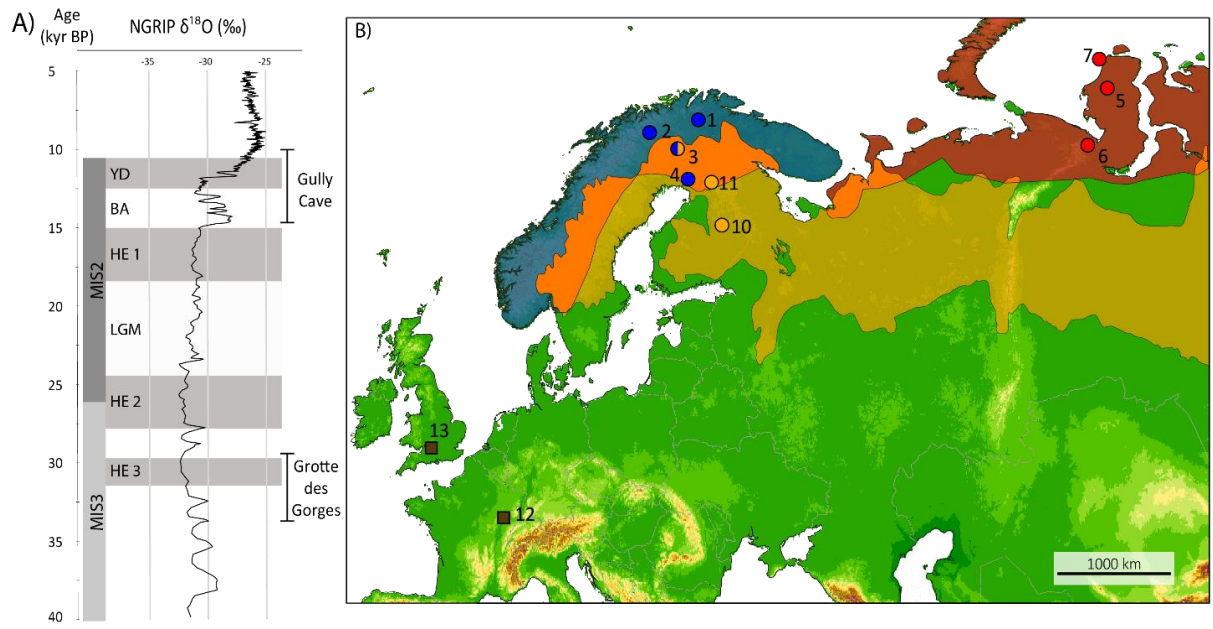


Figure 2

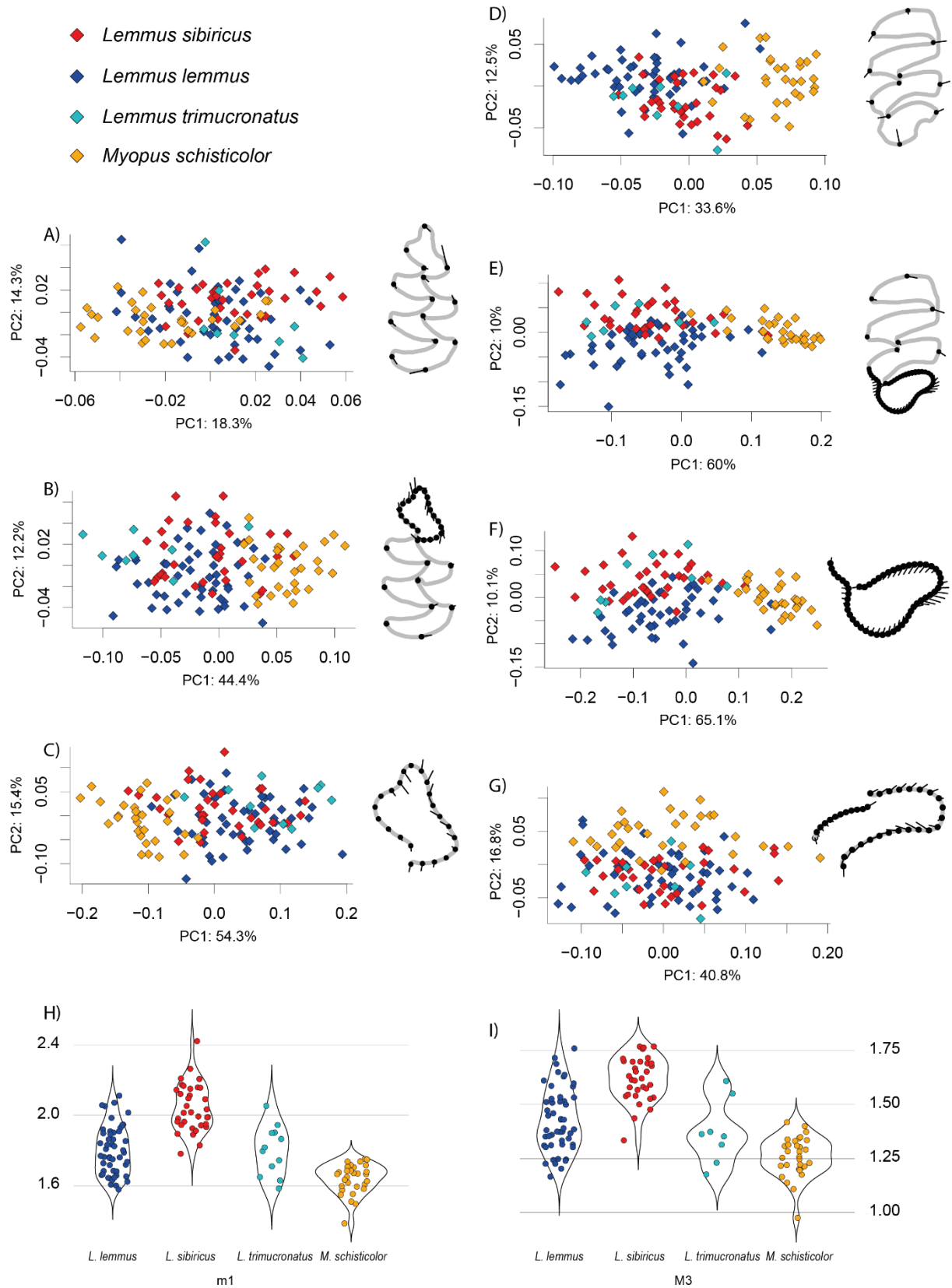


Figure 3

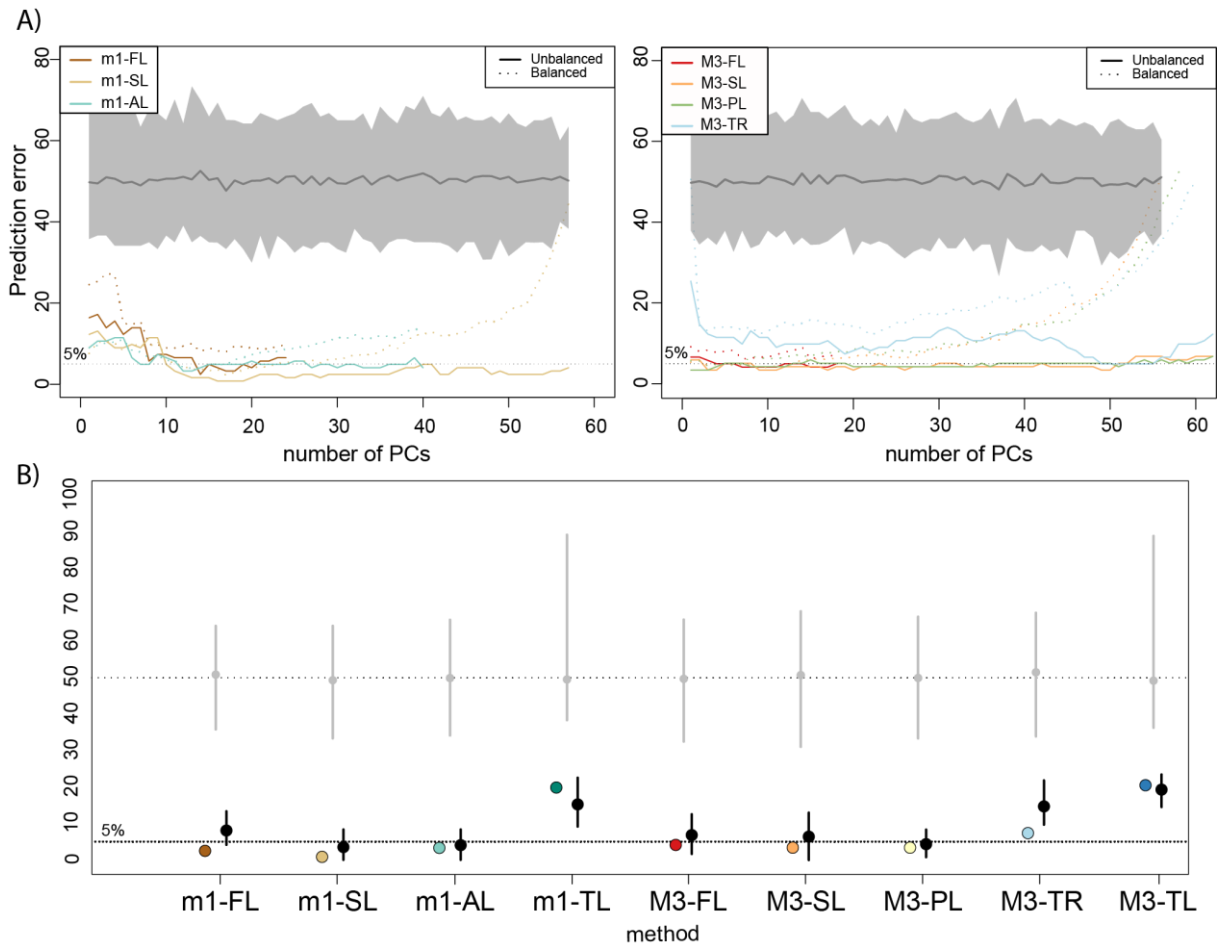


Figure 4



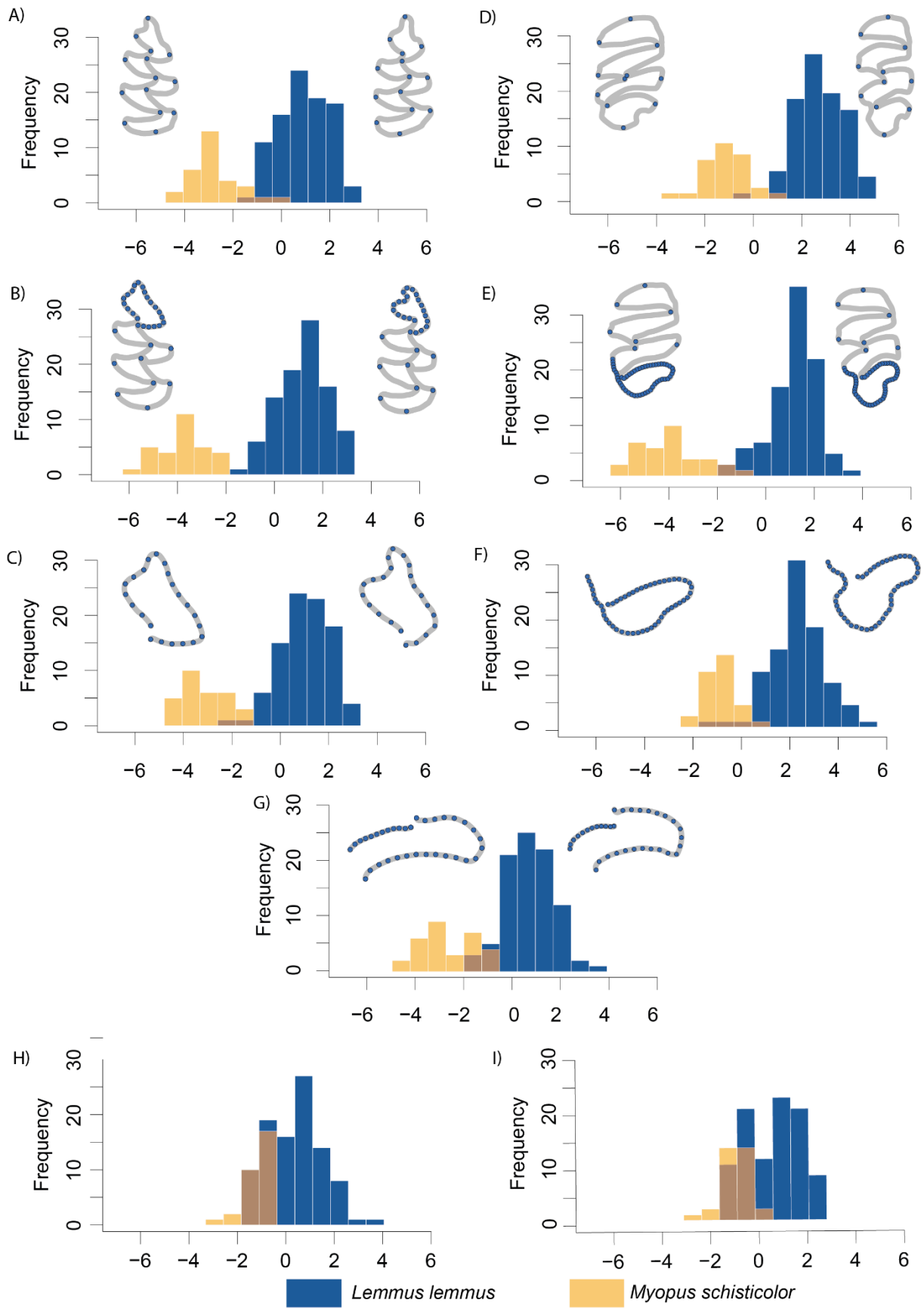


Figure 5

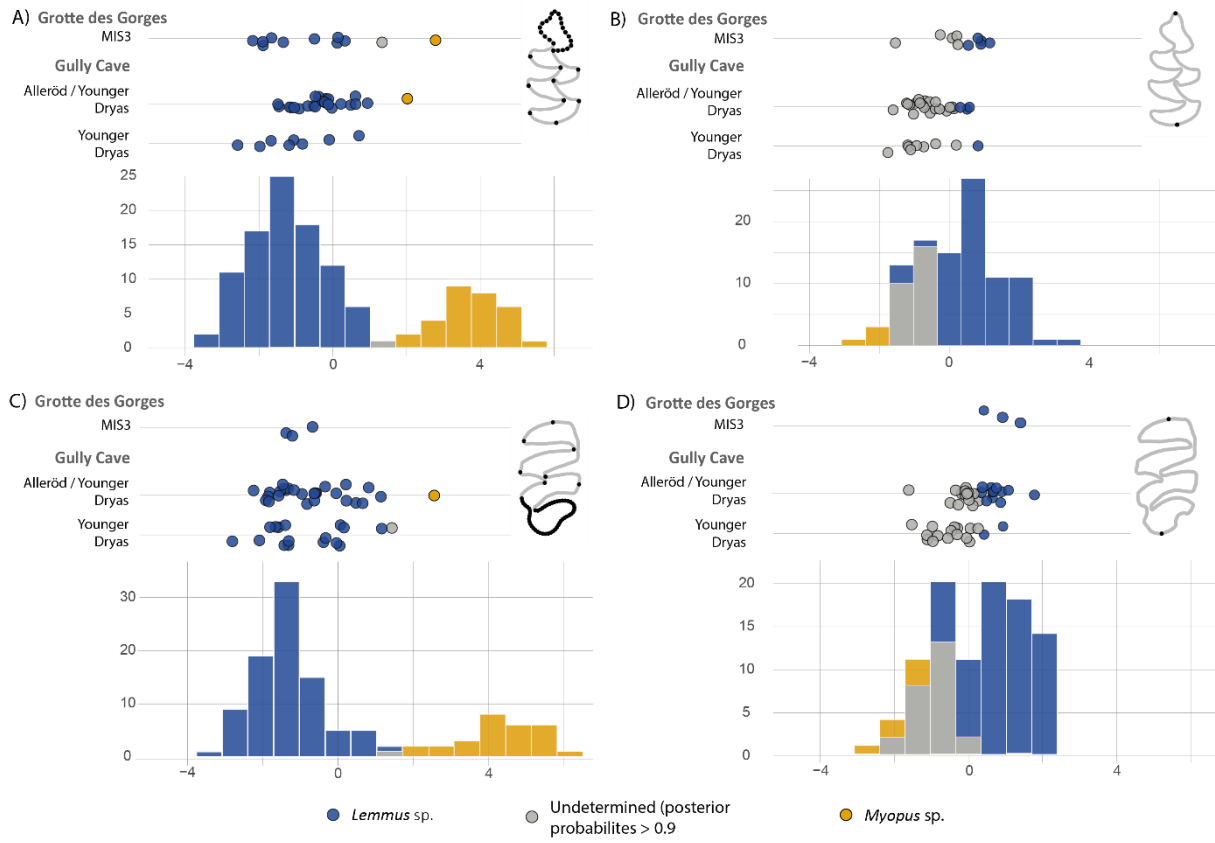


Figure 6

Table 1: List of the analysed specimens with their origin and counts (neighbouring localities are merged). See figure 1 for localities.

	Species	Location	Lower m1	Upper M3
Modern specimens	<i>Lemmus lemmus</i> (50)	1- Karigasniemi	3	3
		2- Kilpisjärvi	15	14
		3- Pallasjärvi, Muonio	11	10
		4- Rovaniemi	21	18
	<i>Lemmus sibiricus</i> (34)	5- Sabetta	9	11
		6- Erkuta	10	10
		7- Bely Island	11	11
		(8)- Wrangel Island	4	1
	<i>Lemmus trimucronatus</i> (12)	(9)-Victoria Island	12	8
	<i>Myopus schisticolor</i> (31)	10-Sotkamo, Valtimo, Kuhmo, Lieka,	20	21

		11-Posio	1	1
		(3)-Pallasjarvi, Muonio	8	8
<b>Fossil specimens</b>	Amange	MIS3	11	3
	Gully Cave (M3: 43 ; m1: 35)	Boundary Allerød / Younger Dryas	23	26
		Younger Dryas	8	17
		Younger Dryas?	4	0

Table 2: Datasets used in the present study. FL = Fixed landmarks, SL= Semi landmarks (including FL and AL for m1 and FL and PL for M3), PL = Posterior loop, AL = Anterior loop, TL = ToothLength.

	Landmark scheme	Number of		Evaluated criteria	Reference
		Landmarks	Semi-landmarks		
<b>M3</b>	FL	11	-	Width of the teeth	Chaline, 1988
	PL	2	50	Complexity of the posterior loop	Ponomarev et al., 2013, Markova et al., 2017
	SL	9	50	Complete shape	-
	TR	4	10 + 20	Depth of A1	Chaline, 1988
				Confluence of FL2	Ponomarev et al., 2013
				Asymmetry of FL2	Markova et al., 2017
TL	2	-	Tooth length	Chaline, 1988	
<b>M1</b>	FL	14	-	Organisation of the buccal triangles	Chaline, 1988
	AL	2	20	Complexity of the anterior loop	Ponomarev et al., 2013, Markova et al., 2017
	SL	11	20	Complete shape	-
	TL	2	-	Tooth length	Chaline, 1988

Table 3: Abbreviations: Tot. PCs= Total Number of PCs, Opt. PCs = Optimal Number of PCs used in the model, PC1+PC2 = cumulative proportion of variance explained by PC1 + PC2, % Opt. class. actual = percentage of prediction error of modern specimens with the optimal number of PCs (see text for details).

	Dataset	Tot. PCs	Opt. PCs	PC1 + PC2	% Pred. Error	% Opt. class. actual	% Opt. class. fossil	Fossil identification	
								<i>Lemmus</i>	<i>Myopus</i>
<b>M1</b>	FL	28	14	32.6	2.5	85.5	80.4	38	8
	SL	62	19	56.6	0.8	95.9	97.8	44	2
	AL	44	12	69.6	3.3	93.4	71.7	27	19
	TL	-	-	-	19.8	41.3	19.6	39	7
<b>M3</b>	FL	18	17	46.1	4.1	89.3	80.4	36	1
	SL	99	26	70	3.4	94.9	100	42	1
	PL	92	3	75.7	3.4	88.1	65.2	22	1
	TR	62	19	57.7	7.3	83.6	76.1	27	5
	TL	-	-	-	20.5	41.8	34.8	13	5

Table 4: Fossil identification for m1 and M3. The number of specimens identified with associated posterior probabilities > 0.9 are in brackets

		m1				M3				
Sites	Genera	<b>m1FL</b>	<b>m1SL</b>	<b>m1AL</b>	<b>m1TL</b>	<b>M3FL</b>	<b>M3SL</b>	<b>M3PL</b>	<b>M3TR</b>	<b>M3TL</b>
Gully Cave (Younger Dryas)	<i>Myopus</i>	0 (0)	0 (0)	3 (3)	3 (0)	2 (0)	0 (0)	2 (0)	1 (1)	3 (0)
	<i>Lemmus</i>	12 (12)	12 (12)	9 (2)	9 (0)	15 (15)	17 (16)	15 (10)	16 (1)	14 (2)
Gully Cave (Allerød-Younger Dryas)	<i>Myopus</i>	6 (4)	1 (1)	13 (9)	3 (0)	2 (1)	1 (1)	10 (6)	3 (1)	1 (0)
	<i>Lemmus</i>	17 (10)	22 (22)	10 (9)	20 (3)	24 (19)	25 (25)	16 (9)	23 (19)	25 (12)
Grotte des Gorges	<i>Myopus</i>	2 (2)	1 (1)	3 (3)	1 (0)	0 (0)	0 (0)	0 (0)	0 (0)	0 (0)
	<i>Lemmus</i>	9 (9)	10 (9)	8 (7)	10 (6)	3 (2)	3 (3)	3 (3)	3 (3)	3 (3)